Bollettino di Geofisica Teorica ed Applicata Vol. 56, n. 4, pp. 461-488; December 2015
DOI 10.4430/bgta0162

Was the Mirandola thrust really involved in the Emilia 2012 seismic sequence (northern Italy)? Implications on the likelihood of triggered seismicity effects

G. Lavecchia [1], R. de Nardis [1,3], G. Costa [2], L. Tiberi [2], F. Ferrarini [1], D. Cirillo [1], F. Brozzetti [1] and P. Suhadolc [2]

[1] *GeosisLab, DiSPUTer, University of Chieti-Pescara "G. d'Annunzio", Campus Universitario, Chieti Scalo, Italy*
[2] *Dipartimento di Matematica e Geoscienze, University of Trieste, Italy*
[3] *Dipartimento della Protezione Civile, Rome, Italy*

(Received: January 30, 2015; accepted: May 4, 2015)

ABSTRACT We present the results of an interdisciplinary study aimed at defining the geometry of the fault segments activated by the Emilia 2012 thrust sequence (M_W up to 6.1), which are located at the front of the Ferrara Arc (northern Italy) and partially overlap with an area undergoing hydrocarbon exploitation since 1980 (Cavone oil field). We relocate 40 well-recorded earthquakes with M_W prevailingly ≥4.0 in the time interval from May 20 to June 12, 2012, plus an event that occurred in a nearby area on July 17, 2011 (M_W 5.0). The geological and seismotectonic setting of the area is discussed, some interpretative geological sections across the hypocentral volumes are elaborated, and the shape of the identified individual seismogenic fault segments is schematically represented as depth contour lines. The resulting earthquake/fault association highlights a rather complex segmentation pattern, with four neighbouring sources involved, all belonging to the SSW-dipping Ferrara Thrust System. The two main events of the Emilia 2012 sequence did not activate the Mirandola thrust underlying the Cavone reservoir, although this thrust was illuminated by some subsidiary activity mainly concentrated close to the hydrocarbon field. The likelihood of triggered seismicity effects due to the extraction/injection activities within the Cavone oil field are discussed.

Key words: Emilia 2012 seismic sequence, northern Italy, thrust earthquakes, hydrocarbon field, earthquake relocation, structural style, seismotectonics, triggering effects.

1. Introduction

On May 2012, an intense seismic sequence with two main moderate earthquakes [May 20: I_0 VII MCS, M_L 5.9, M_W 6.1; May 29: I_0 VII MCS, M_L 5.8, M_W 6.0: Pondrelli *et al.* (2012)] was generated by thrust faulting in the Ferrara Arc, at the Padan buried front of the northern Apennines Outer Thrust System (Emilia region, northern Italy) (Figs. 1a and 1c). The sequence produced widespread damage (Galli *et al.*, 2012; Tertulliani *et al.*, 2012), partly due to shear-

wave-amplification effects caused by the unconsolidated sediments in the Po alluvial plain (Malagnini *et al.,* 2012; de Nardis *et al*., 2014; Milana *et al*., 2014). The epicentral area of the Emilia 2012 earthquakes was characterized by modest historical and instrumental seismicity (M_W<5) (Rovida *et al.,* 2011; Burrato *et al*., 2012) and by extensive drilling campaigns for oil and gas exploration purposes (Casero, 2004) (Fig. 1a). For this reason, soon after the second main event of May 29, a question arose about the possible role of the extraction and/or injection activities in the nearby Cavone oil field (Mirandola exploitation license) in inducing/triggering the 2012 seismic activity. Two international technical-scientific commissions investigated the problem, using a multidisciplinary geological-seismological, statistical, and/or geo-mechanical approach (Astiz *et al*., 2014; ICHESE, 2014). They both agreed to exclude a case of induced seismicity, with this term referring to a seismic process entirely controlled by a non-tectonic phenomenon, typically occurring within an aseismic area (Cesca *et al*., 2013b). Conversely, they reached partially different conclusions regarding the triggered component, referring to transient Coulomb failure stress changes capable of promoting the rupture process on the faults. According to Astiz *et al*. (2014), the fluid pressure increase/decrease linked with the Cavone activities were too localized and negligible to produce any triggering effect at the sources of both the May 20 and 29 main events. According to ICHESE (2014), a triggering component might be hypothesized in the May 20 case, in light of a statistical correlation between the seismic activity and an injection pressure increase within one of the deep Cavone wells, which, according to their geometric reconstruction, was in hydraulic contact with the seismogenic source.

The Astiz *et al*. (2014) and ICHESE (2014) geometric reconstructions of the Emilia 2012 fault system, which were at the base of their evaluation of the triggered effects, are substantially different, but share the fundamental seismogenic role attributed to the Mirandola thrust, located beneath the Cavone reservoir. As a matter of fact, the Mirandola thrust was largely interpreted (Bignami *et al*., 2012; Burrato *et al*., 2012; Marzorati *et al*., 2012; Scognamiglio *et al*., 2012; Tizzani *et al*., 2013; Ventura and Di Giovambattista, 2013; Govoni *et al*., 2014) as the most likely source of the May 29 event for two main reasons: 1) it was already well known in the literature as an active and possibly seismogenic thrust of the Ferrara Arc (Carminati *et al*., 2010; DISS Working Group, 2015); 2) it was located just beneath the May 29 epicentral area. This hindered the search for alternative solutions, even if a vertical mismatch of ~5 km between the Mirandola thrust and the May 29 hypocentre was soon evident. In fact, the earliest locations (ISIDe Working Group INGV, 2015), later on confirmed by more detailed data (Chiarabba *et al*., 2014; Govoni *et al*., 2014), provided a depth of 9-10 km for the May 29 main event hypocentre, whereas on the same vertical line the Mirandola thrust, as previously interpreted from seismic line and deep wells data (Massoli *et al*., 2006; Martelli and Molinari, 2008; Toscani *et al*., 2009), was positioned at depths of about 5 km.

In this paper, based on accurate earthquake locations and on fault geometry interpretation, we support a different hypothesis (Lavecchia *et al*., 2012), which excludes involvement of the Mirandola thrust in the nucleation of the two main May 20 and 29 events of the Emilia 2012 sequence. These events are instead associated with the activation of a complex pattern of interconnected individual fault segments, all belonging to the Ferrara Thrust System. The Mirandola thrust was only subordinately activated, in the close surroundings of the Cavone field. The spatial relationships between the newly defined individual sources and the regions

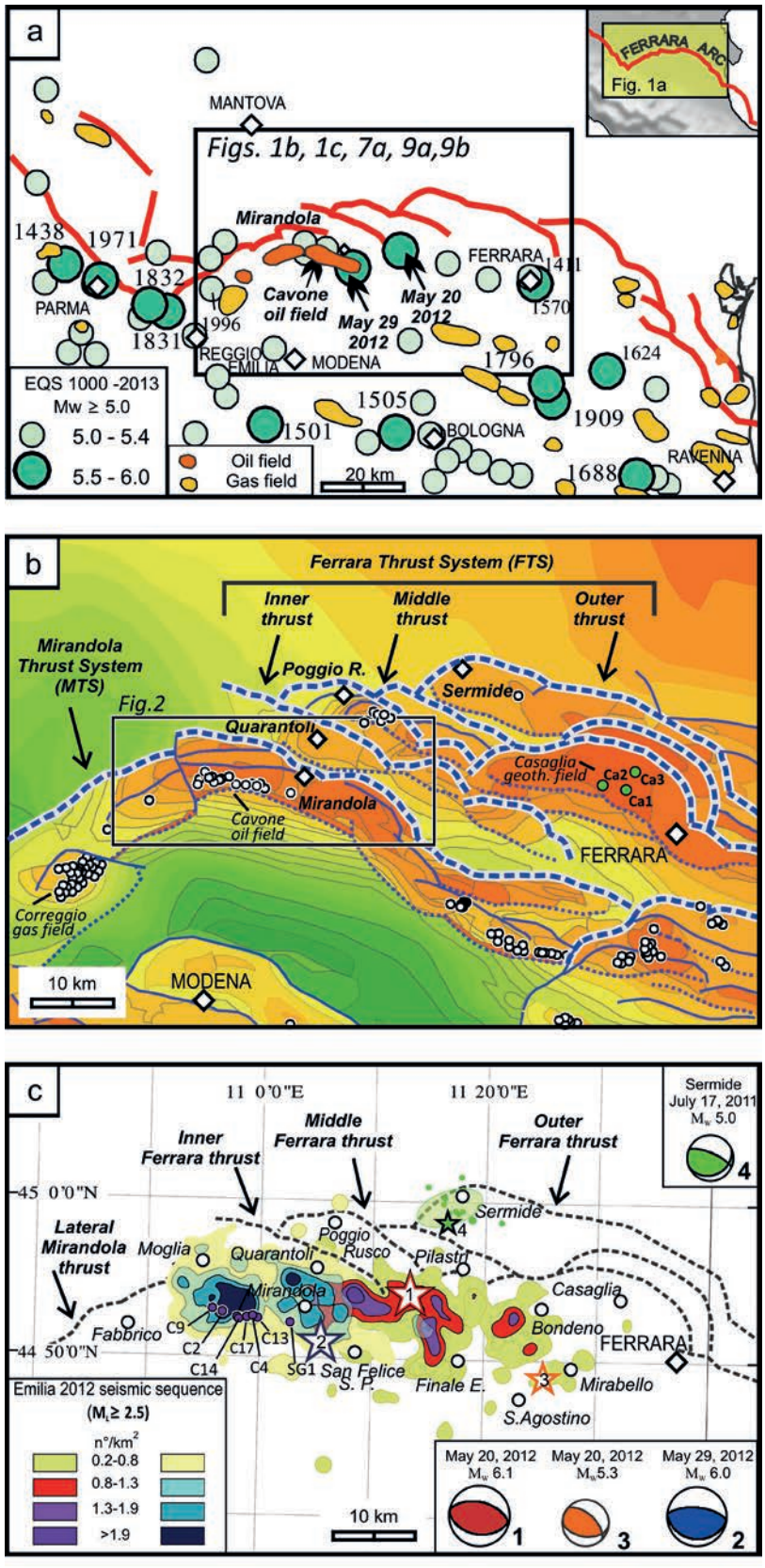

Fig. 1 - Seismotectonic setting of the Emilia 2012 seismic sequence: a) historical and instrumental earthquakes with $M_W \geq 5.0$ that occurred in the time interval 1000 - 2013 from CPTI11 (Rovida *et al.*, 2011; ISIDe Working Group INGV, 2015) and boundaries of the oil and gas fields from Casero (2004); red line represents the outer Quaternary front of the northern Apennines Thrust System; b) Plio-Quaternary compressional structures with foredeep deposits decreasing in thickness from dark green (~7 km) to orange (~1 km), from the Structural Model of Italy, scale 1:500,000 (CNR - P.F. Geodinamica, 1990). Key: dashed lines = major Quaternary thrust fronts; continuous lines = other thrusts; dotted lines = back-thrusts and syn-compressional south-dipping normal faults. The white dots represent hydrocarbon drilling sites extracted from ViDEPI Project (2014) (see Fig. 2 for further details) and the green dots Ca1, Ca2, Ca3 refer to the Casaglia geothermal field. c) Epicentral area of the Emilia 2012 sequence from ISIDe database (ISIDe Working Group INGV, 2015) represented as density contours of earthquake locations in the time intervals from May 15 to 28, 2012, and from May 29 to June 15, 2012. Stars 1 and 2 represent the epicentres of two main events (May 20 and 29) of the Emilia 2012 sequence (e.g., EQ1 and EQ2 in this paper); star 3 is the largest event (May 20) recorded within the eastern area of the epicentral sequence (event n. 10 in Table 1); star 4 represents the major event of the small neighbouring sequence that occurred in 2011. Focal mechanisms are from Pondrelli *et al.* (2012). The Cavone field wells operating in 2012 for extraction and water disposal are highlighted as purple dots (from ICHESE, 2014).

of stress perturbations due to extraction/injection activities within the Cavone oil field will be described and their implications regarding the likelihood of triggered earthquake activity discussed.

Table 1 - Hypocentral parameters of 41 relocated earthquakes that occurred in Emilia 2012 seismic sequence (northern Italy) during the period May 20 to June 12, 2012, plus one event that occurred in the same area on July 17, 2011 (M_L 4.8, M_W 5.0). The hypocentral data were computed from travel times manually measured from the digital seismograms and computed with HYPOELLIPSE code (Lahr, 1999), and the vertically stratified earth models specified in the text and in Fig. 4. M_L* and M_W* are derived from ISIDe database (ISIDe Working Group INGV, 2015) and Gallo *et al.* (2014), respectively.

	Model A								Model D								Model F								M	
ID	Date	Time	Lon	Lat	depth	rms	ErrH	ErrZ	Date	Time	Lon	Lat	depth	rms	ErrH	ErrZ	Date	Time	Lon	Lat	depth	rms	ErrH	ErrZ	ML*	MW*
1	20110717	18.30.26	11.280	44.988	-4.2	0.3	0.6	0.7	20110717	18.30.26	11.275	44.995	-2.1	0.3	0.5	0.6	20110717	18.30.27	11.287	44.995	-2.6	0.3	0.5	1.2	4.8	5.0
2	20120520	02.03.51	11.218	44.907	-5.3	0.3	0.4	0.7	20120520	02.03.52	11.217	44.913	-4.0	0.3	0.4	0.5	20120520	02.03.51	11.230	44.913	-2.9	0.4	0.4	0.7	5.9	6.1
3	20120520	02.07.30	11.330	44.829	-8.6	0.9	0.7	1.6	20120520	02.07.31	11.326	44.830	-8.3	0.9	0.5	3.4	20120520	02.07.31	11.338	44.831	-6.1	0.8	0.6	1.6	5.1	4.5
4	20120520	02.11.45	11.304	44.859	-7.0	0.2	0.6	2.1	20120520	02.11.46	11.299	44.862	-5.7	0.2	0.6	1.0	20120520	02.11.46	11.316	44.868	-3.7	0.1	0.6	0.9	4.3	3.6
5	20120520	02.12.41	11.201	44.880	-7.9	0.3	1.0	2.4	20120520	02.12.42	11.209	44.885	-4.5	0.3	0.7	1.0	20120520	02.12.42	11.222	44.886	-4.6	0.3	0.9	1.9	4.3	4.2
6	20120520	02.21.52	11.132	44.868	-6.9	0.2	0.5	0.4	20120520	02.21.53	11.135	44.872	-6.4	0.2	0.5	0.4	20120520	02.21.52	11.135	44.871	-7.2	0.2	0.5	0.5	4.1	4.4
7	20120520	02.39.08	11.213	44.881	-6.2	0.1	1.5	3.0	20120520	02.39.09	11.217	44.895	-5.6	0.1	1.1	2.5	20120520	02.39.09	11.226	44.896	-5.7	0.0	1.5	2.6	4.0	4.1
8	20120520	03.02.48	11.101	44.872	-9.2	0.3	0.5	0.8	20120520	03.02.49	11.098	44.880	-10.9	0.3	0.6	1.0	20120520	03.02.49	11.100	44.877	-9.2	0.3	0.5	0.8	4.9	5.3
9	20120520	09.13.20	11.203	44.878	-10.2	0.4	0.6	0.6	20120520	09.13.21	11.212	44.884	-9.9	0.3	0.6	1.0	20120520	09.13.21	11.207	44.880	-10.3	0.4	0.6	0.5	4.2	4.6
10	20120520	13.18.02	11.425	44.813	-10.8	0.5	0.4	3.6	20120520	13.18.01	11.418	44.829	-5.5	0.4	0.4	0.7	20120520	13.18.02	11.417	44.823	-3.2	0.4	0.4	1.0	5.1	5.3
11	20120520	17.37.12	11.308	44.879	-5.0	0.4	0.4	0.9	20120520	17.37.13	11.304	44.883	-2.6	0.4	0.4	0.7	20120520	17.37.13	11.312	44.886	-3.1	0.4	0.4	0.8	4.5	4.9
12	20120521	16.37.30	11.322	44.862	-5.8	0.2	0.5	0.5	20120521	16.37.31	11.329	44.865	-4.8	0.3	0.4	0.5	20120521	16.37.31	11.325	44.864	-6.7	0.3	0.4	0.6	4.1	4.4
13	20120522	09.31.13	11.229	44.856	-7.1	0.2	0.3	5.5	20120522	09.31.14	11.240	44.859	-6.7	0.2	0.3	0.4	20120522	09.31.14	11.236	44.860	-8.0	0.2	0.3	0.5	3.8	--
14	20120523	21.41.17	11.242	44.844	-9.2	0.4	0.2	0.5	20120523	21.41.18	11.253	44.847	-8.6	0.4	0.3	0.6	20120523	21.41.18	11.250	44.847	-8.9	0.3	0.3	0.5	4.3	4.5
15	20120525	10.31.21	11.217	44.846	-9.3	0.2	0.2	0.6	20120525	10.31.22	11.227	44.849	-8.3	0.2	0.3	0.6	20120525	10.31.22	11.223	44.849	-8.7	0.2	0.2	0.5	3.9	0.0
16	20120525	13.14.03	11.098	44.865	-6.1	0.2	0.2	0.2	20120525	13.14.04	11.100	44.870	-5.8	0.2	0.3	0.2	20120525	13.14.04	11.098	44.868	-5.2	0.2	0.2	0.5	4.0	4.2
17	20120526	21.07.30	11.171	44.830	-11.3	0.2	0.3	0.3	20120526	21.07.31	11.179	44.832	-10.6	0.2	0.3	0.6	20120526	21.07.31	11.176	44.833	-10.8	0.2	0.3	0.5	3.8	--
18	20120527	18.18.44	11.171	44.854	-5.8	0.2	0.2	0.3	20120527	18.18.45	11.177	44.857	-5.7	0.3	0.2	0.3	20120527	18.18.45	11.174	44.858	-4.4	0.3	0.2	0.3	4.0	4.5
19	20120527	20.25.41	11.170	44.865	-6.5	0.2	0.4	0.4	20120527	20.25.42	11.177	44.868	-6.2	0.2	0.4	0.4	20120527	20.25.42	11.174	44.870	-7.0	0.2	0.3	0.8	3.8	0.0
20	20120529	07.00.02	11.069	44.842	-8.8	0.3	0.3	0.6	20120529	07.00.03	11.070	44.848	-8.6	0.3	0.3	0.7	20120529	07.00.02	11.070	44.847	-8.7	0.3	0.3	0.6	5.8	5.8
21	20120529	07.07.18	11.018	44.863	-4.4	0.2	2.4	3.2	20120529	07.07.20	11.017	44.863	-3.4	0.2	0.4	0.9	20120529	07.07.20	11.030	44.868	-3.0	0.2	0.5	1.6	4.0	--
22	20120529	07.49.26	11.138	44.856	-7.3	0.1	0.3	0.5	20120529	07.49.27	11.145	44.861	-6.7	0.1	0.3	0.2	20120529	07.49.27	11.140	44.861	-7.3	0.1	0.3	0.4	3.7	--
23	20120529	08.15.08	11.090	44.863	-7.8	0.1	0.3	0.7	20120529	08.15.09	11.092	44.868	-7.2	0.1	0.4	0.7	20120529	08.15.09	11.092	44.866	-7.7	0.1	0.3	0.4	3.8	--
24	20120529	08.25.50	10.970	44.868	-9.4	0.2	0.3	0.5	20120529	08.25.51	10.963	44.875	-9.0	0.2	0.3	0.7	20120529	08.25.51	10.966	44.874	-9.4	0.1	0.3	0.5	4.5	4.7
25	20120529	08.27.21	11.057	44.882	-6.2	0.2	0.4	0.3	20120529	08.27.22	11.057	44.888	-5.7	0.2	0.5	0.3	20120529	08.27.22	11.055	44.889	-6.2	0.2	0.4	0.4	4.7	4.4
26	20120529	08.40.56	10.993	44.856	-9.8	0.1	0.4	0.5	20120529	08.40.57	10.986	44.862	-10.3	0.1	0.4	1.0	20120529	08.40.57	10.992	44.861	-9.7	0.1	0.4	0.5	4.2	4.5
27	20120529	09.30.20	11.091	44.854	-8.3	0.1	0.3	0.5	20120529	09.30.21	11.093	44.858	-7.6	0.1	0.3	0.5	20120529	09.30.20	11.092	44.857	-7.8	0.1	0.3	0.3	4.2	4.2
28	20120529	10.55.55	11.007	44.861	-9.7	0.2	0.3	0.5	20120529	10.55.56	11.003	44.868	-9.9	0.2	0.3	0.6	20120529	10.55.56	11.005	44.867	-9.8	0.1	0.3	0.4	5.3	5.5
29	20120529	11.00.23	10.953	44.893	-8.3	0.2	0.4	1.0	20120529	11.00.24	10.946	44.900	-7.1	0.1	0.5	1.1	20120529	11.00.24	10.950	44.900	-8.2	0.2	0.4	0.7	5.2	--
30	20120529	11.00.00	10.956	44.859	-6.9	0.3	0.3	0.9	20120529	11.00.01	10.951	44.866	-7.5	0.3	0.3	1.4	20120529	11.00.01	10.954	44.864	-8.0	0.3	0.3	0.4	4.9	4.4
31	20120529	14.39.39	11.043	44.882	-6.2	0.1	0.4	0.3	20120529	14.39.40	11.043	44.888	-5.8	0.1	0.4	0.3	20120529	14.39.40	11.045	44.889	-5.2	0.1	0.4	0.5	3.9	--
32	20120529	18.27.59	10.946	44.890	-8.2	0.2	0.3	0.9	20120529	18.28.00	10.939	44.895	-6.9	0.1	0.5	0.5	20120529	18.28.00	10.942	44.897	-8.3	0.2	0.4	0.6	3.9	--
33	20120529	18.44.40	11.114	44.865	-6.3	0.1	0.4	0.3	20120529	18.44.41	11.116	44.867	-5.8	0.0	0.3	0.3	20120529	18.44.41	11.113	44.867	-5.3	0.1	0.3	0.7	3.2	--
34	20120531	14.58.20	10.897	44.873	-10.0	0.1	0.9	0.8	20120531	14.58.21	10.877	44.883	-8.3	0.1	1.1	2.6	20120531	14.58.20	10.883	44.880	-10.0	0.1	1.0	1.1	4.0	4.2
35	20120531	19.04.02	10.999	44.880	-8.3	0.1	0.3	0.4	20120531	19.04.04	10.995	44.888	-7.6	0.1	0.3	0.5	20120531	19.04.03	10.998	44.887	-8.5	0.1	0.3	0.4	4.2	4.4
36	20120603	19.20.42	10.963	44.895	-5.8	0.4	0.4	0.6	20120603	19.20.43	10.954	44.906	-7.9	0.4	0.4	1.3	20120603	19.20.43	10.956	44.906	-8.1	0.4	0.4	1.1	5.1	5.1
37	20120604	06.55.48	10.984	44.883	-9.4	0.1	0.4	0.7	20120604	06.55.49	10.979	44.889	-8.7	0.1	0.4	0.8	20120604	06.55.49	10.981	44.890	-9.2	0.1	0.4	0.6	3.8	--
38	20120605	03.11.35	11.083	44.865	-7.9	0.1	0.7	0.5	20120605	03.11.36	11.089	44.873	-7.7	0.1	0.7	0.6	20120605	03.11.36	11.089	44.875	-7.7	0.1	0.7	0.6	2.7	--
39	20120609	13.25.14	11.100	44.871	-6.3	0.2	0.5	0.3	20120609	13.25.15	11.108	44.883	-5.8	0.2	0.4	0.4	20120609	13.25.15	11.112	44.881	-5.6	0.2	0.5	0.7	3.4	--
40	20120612	01.48.35	10.944	44.886	-10.1	0.1	0.3	0.4	20120612	01.48.36	10.937	44.895	-10.1	0.1	0.3	0.5	20120612	01.48.36	10.941	44.893	-10.6	0.1	0.3	0.3	4.3	4.5
41	20120612	15.56.01	10.943	44.905	-7.8	0.1	0.5	1.0	20120612	15.56.02	10.938	44.914	-7.4	0.1	0.6	0.9	20120612	15.56.02	10.938	44.917	-8.2	0.1	0.6	0.7	3.4	--

2. The Ferrara Arc

2.1. Tectonic setting

The Ferrara Arc is an active NNE-verging fold-and-thrust zone at the front of the Apennine compressional belt (Boccaletti *et al.*, 2011). From west to east, its frontal thrust rotates in strike from WSW-ENE to W-E and NW-SE (Fig. 1a). In the western and central portions, the Ferrara Arc is composed of two first-order blind thrust systems (Fig. 1b). From south to north, they are the arcuate and north-convex Mirandola Thrust System (MTS) and the mostly linear, WNW-ESE striking Ferrara Thrust System (FTS), separated for a large portion by a broad syncline filled by Lower Pliocene-Lower Pleistocene sediments. The MTS, which contains in its apical sector the Cavone anticline, is mostly continuous along strike for its overall extent (Picotti and Pazzaglia, 2008; Ghielmi *et al.*, 2010). The FTS, which represents the outermost compressional system at the front of the northern Apennine belt, is articulated into a number of second-order NNE-verging fold-and-thrust structures, generally referred to as Inner, Middle and Outer Ferrara thrusts (Fig. 1b, CNR - P.F. Geodinamica, 1990). The Middle Ferrara Thrust is especially complex and along-strike subdivided into two major fold-and-thrust structures, here referred to as Poggio Rusco and Casaglia segments (Fig. 1c).

The MTS and the FTS differ slightly in their deformation age, the first mainly starting to nucleate during the Late Pliocene and the second during the Early Pleistocene (Ghielmi *et al.*, 2010). By the Middle Pleistocene, at about 0.6 My, the thrust front of the Ferrara Arc had reached its present position, but an ongoing N-S compression in the region is verifiable by seismological and geodetic data (Devoti *et al.*, 2011; Montone *et al.*, 2012). Namely, historical and instrumental earthquakes (Fig. 1a) show the activity of 1) the WSW-ENE side of the Ferrara Arc, coinciding with the western lateral ramp sector of the MTS, where the 1831 and 1832 (M_W 5.5) and the Reggio Emilia 1996 (M_W 5.4) earthquakes occurred; 2) the central nearly E-W striking portion of the arc, substantially coinciding with the FTS, activated by the Emilia 2012 sequence (M_W up to 6.1) and, possibly, by the Ferrara 1570 (M_W 5.5) earthquake and 3) the eastern NW-SE side of the arc, where the Argenta 1624 (M_W 5.5) earthquake nucleated. The focal mechanisms of the instrumental events show prevailing dip-slip reverse kinematics across the Ferrara Arc frontal sector and a prevailing strike-slip component along the WSW-ENE side of the arc, which plays the role of a left-lateral ramp (Selvaggi *et al.*, 2001).

2.2. Hydrocarbon and geothermal fields

The Ferrara Arc is a site of relatively large and economically significant hydrocarbon and geothermal resources in Italy (Fig. 1a). They were discovered and/or exploited since 1950 in the Correggio gas field, since 1956 in the Casaglia geothermal field, and since 1980 in the Cavone oil field (ICHESE, 2014 and references therein); a minor gas field was discovered since 1960 at Poggio Rusco (Fig. 1b). The Cavone and Casaglia fields were both drilled within fractured Mesozoic carbonate reservoirs, at depths of about 2.5-3.0 and 1.2-2.0 km, respectively. The Correggio and Poggio Rusco gas fields were encountered in the Pliocene, at a depth of about 1.0-1.2 km.

The Poggio Rusco gas field and the Casaglia geothermal field are both located within anticline structures at the hanging wall of the Middle Ferrara Thrust (Fig. 1b). The Correggio and Cavone fields are located in a more internal structural position, within hanging-wall

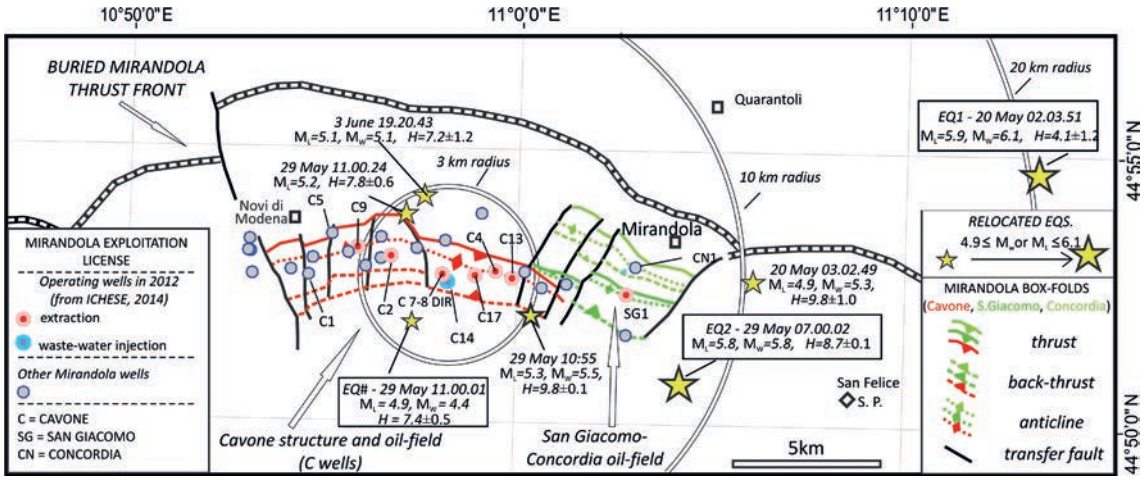

Fig. 2 - Structural detail of the Cavone box fold (after Carminati *et al*., 2010) with the location of the Mirandola license wells (ViDEPI Project, 2014) and of the wells operating in 2012 before the seismic sequence onset (from ICHESE, 2014). The epicentres of the major events of the Emilia 2012 sequence (M_L or M_W ≥4.9), relocated in this paper (Table 1) are also reported. Circumference arcs with radii of 3, 10, and 20 km centred on the C14 injection well are shown. M_L and M_W are derived from ISIDe Working Group INGV (2015) and Gallo *et al*. (2014), respectively.

anticlines at the MTS front (Fig. 1b). The Correggio anticline is located along the WSW-ENE striking MTS sector, whereas the Cavone anticline is located in the apical, nearly E-W striking, MTS sector and is overthrusted on another small *en echelon* anticline, which contains the San Giacomo and Concordia oil fields (Fig. 2). The Cavone, San Giacomo, and Concordia fields are included in the Mirandola exploitation license, and as a whole depict a large, long (~15.0 km) and narrow (~1.5 km) asymmetric, north-verging fold-and-thrust anticline. This structure is slightly arcuate northwards, rotating in strike from about N80°E in the west to about N110°E in the east (Carminati *et al*., 2010). The Mirandola anticline has been largely explored and drilled by a large number of deep wells, up to a maximum depth of 5507 m in the Cavone 1 well and of 5000 m in the Concordia 1 well. The Cavone reservoir produces a heavy oil (20°-23° API) rich in sulphur (3-4%) (Nardon *et al*., 1990), and has had an average yearly production during the last seven years of 30,000 tons (ViDEPI Project, 2014). The carbonate reservoir lithotypes are represented by the Lower Jurassic shelf limestones of the Calcari Grigi di Noriglio Fm. and the Lower Cretaceous Brecce di Cavone Fm. (Nardon *et al*., 1990), located at a minimum depth of 2500 m, with an average thickness of 400-700 m (ICHESE, 2014). The age of the source rock is uncertain, probably Triassic (Anelli *et al*., 1996).

Whereas the Correggio and Casaglia field are located tens of kilometres outwards from the Emilia 2012 epicentral area, the Cavone oil fields completely overlaps with the May 29 aftershock sequence (Fig. 2). Many wells were operating in 2012 (ICHESE, 2014). Among these, Cavone 2 (depth 4096 m), producing oil with some intervals of inactivity since 1980, Cavone 13 (depth 3310 m), producing oil since December 1987, and Cavone 14 (depth 3400 m) performing water-disposal re-injection since January 1993 (see C2, C3, C14 in Fig. 2). This spatial configuration soon opened the question of the likelihood of exploitation-injection having triggered, or even induced, seismicity in the Emilia 2012 sequence.

3. The Emilia 2012 seismic sequence

The Emilia 2012 thrust sequence was associated with the two major events of May 20 [M_W 5.9 in Scognamiglio *et al.* (2012); M_W 6.1 in Pondrelli *et al.* (2012) and Gallo *et al.* (2014)] and May 29 [M_W 5.7 in Scognamiglio *et al.* (2012); M_W 5.8 in Gallo *et al.* (2014) and M_W 6.0 in Pondrelli *et al.* (2012)] and with other six events with M_L and/or M_W ≥5.0 (ns. 3, 8, 10, 20, 28, 29 in Table 1). From now on, we refer to the two major events as EQ1 and EQ2.

The overall Emilia 2012 sequence extended for about 50 km, with an average strike of N100°E, over the central portion of the MTS and the western and central portion of the FTS (Fig. 1c) (Lavecchia *et al.*, 2012; Pezzo *et al.*, 2013; Gallo *et al.*, 2014). The sequence was preceded by a foreshock (M_W 4.1), nucleated on May 19 close to the EQ1 hypocentre, and anticipated by a minor north-verging thrust sequence (M_W 5.0), which occurred on July 17, 2011, a few kilometres northwards, close to the locality of Sermide on the FTS front. The time-space distribution of the aftershock sequence, from May 20 to June 12, highlights two distinct left-stepping *en echelon* epicentral areas, overlapping in between the small localities of Quarantoli and San Felice sul Panaro (see the density contour lines of the number of events with M_L ≥2.5 in Fig. 1c); a minor third cluster may be distinguished eastwards of Finale Emilia.

The hypocentral depths calculated in the literature for the two main events range between 4 and 7 km for EQ1 and between 8 and 13 km for EQ2 (Marzorati *et al.*, 2012; Chiarabba *et al.*, 2014; Govoni *et al.*, 2014; ICHESE, 2014; ISIDe Working Group INGV, 2015; this study). The overall aftershock sequence is mainly confined within the uppermost 11 km (Govoni *et al.*, 2014). Focal mechanisms for the two main events and their major aftershocks, as determined by various authors (Malagnini *et al.*, 2012; Pondrelli *et al.*, 2012; Saraò and Peruzza, 2012; Scognamiglio *et al.*, 2012), show no substantial differences. They imply a nearly sub-horizontal NNE-SSW trending P-axis, which is also coherent with geodetic data (Devoti, 2012). The preferential seismic plane strikes about WNW-ESE for EQ1 and about E-W for EQ2.; the dip angles range from 25° to 35° for EQ1 and from 25° to 30° for EQ2, the only exception being the INGV-ICT solutions that provide greater dip angles (45° and 38°, respectively) (Cesca *et al.*, 2013a).

The EQ1 source was commonly associated (Pezzo *et al.*, 2013; Astiz *et al.*, 2014; Govoni *et al.*, 2014) with the shear thrusting on the middle segment of the FTS (Fig. 1b), whereas the association of EQ2 fault source was less clear and more controversial. Some authors, mainly basing their arguments on geodetic data inversion, associated it with shallow thrusting (~5 km) on the MTS segment located just beneath the Cavone reservoir (Bignami *et al.*, 2012; Burrato *et al.*, 2012). Others, mainly arguing on the basis of earthquake locations and/or of structural analysis, suggested a link with a deeper high-angle segment of the Mirandola basal thrust (Astiz *et al.*, 2014; Bonini *et al.,* 2014; Govoni *et al.*, 2014), with the innermost fault segments of the FTS (Quarantoli thrust in Fig. 1b) (Lavecchia *et al.*, 2012), or, alternatively, with a blind high-angle thrust located beneath the Cavone reservoir within the Mirandola thrust footwall volume (ICHESE, 2014).

4. Emilia 2012 earthquake relocation

The Emilia seismic sequence occurred within the Padan Plain sedimentary basin, which contains a remarkable thickness (up to about 8 km) of Pliocene-Quaternary foredeep deposits

overlain by recent alluvial sediments. Such a geological setting makes the near-source waveforms particularly complex because of the interference of body and locally generated surface waves with the consequent difficulties in reading S-wave arrival times at the closest stations (de Nardis *et al.*, 2014). Moreover, it could make the use of regional velocity models unsuitable for describing this geological context. In order to contribute with our own data to the discussion on the Emilia 2012 individual seismogenic sources, we focused on locating selected major events, based on the analysis of available and well-constrained waveforms.

We determined the arrival times of 40 well-constrained earthquakes mostly with $M_W \geq 4.0$, that occurred during the Emilia 2012 seismic sequence (max M_W 6.1) in the time interval from May 20 to June 12, 2012, plus the event that occurred in the same area on July 17, 2011 (M_L 4.8, M_W 5.0). Specifically, we collected and analyzed the waveforms of events recorded by the permanent and temporary stations of the Italian strong motion network RAN (Gorini *et al.*, 2010; Zambonelli *et al.*, 2011; de Nardis *et al.*, 2014), carefully merging them with the available recordings from ISIDe database (ISIDe Working Group INGV, 2015) and the ones recorded by the Central and Eastern European Earthquake Research Network (jointly managed by the Mathematical and Geosciences Department of the University of Trieste, the National Institute of Oceanography and Experimental Geophysics in Trieste, the Environmental Agency of the Republic of Slovenia, the Zentralanstalt für Meteorologie und Geodynamik in Vienna, and the Croatian Seismological Service in Zagreb).

The integrated database contains more than 900 waveforms (3 channels) recorded at epicentral distances ranging from 4 to 210 km and recorded by 164 stations. In order to overcome the possible difficulties in the detection of S-waves' arrivals, all the available waveforms were visually inspected and a manual picking was performed. The whole data set comprises 546 P- and 244 S-phases, associated with the most significant events of the seismic sequence. A standard weighting scheme was applied, assigning to each P- or S-arrival a weight, varying from 0 (uncertainty of 0.1 s) to 4 (uncertainty greater than 2.0 s). Considering the time readings of both the P-and S-phases, a modified Wadati method (Chatelain, 1978) was adopted in order to: 1) test the reliability and consistency of P-and S-phases; 2) have a rough evaluation of the mean velocity ratio V_P/V_S. From the Wadati plot (Fig. 3), a V_P/V_S ratio of 1.82, with a 95% confidence interval having a squared correlation coefficient (*R2*) greater than 0.98, was estimated. This value of the V_P/V_S ratio is higher than the ones (V_P/V_S = 1.73, V_P/V_S = 1.78 and V_P/V_S = 1.79) obtained, respectively, by Costa *et al.* (1992), Zollo *et al.* (1995), Massa *et al.* (2013) and lower than the one (V_P/V_S = 1.90) proposed by Govoni *et al.* (2014).

The final location of the entire data set was performed using the Hypoellipse code (Lahr, 1999). Specifically, the P- and S- onsets were inverted considering five P-wave velocity models optimized for the study area (Costa *et al.*, 1992; Zollo *et al.*, 1995; Bragato *et al.*, 2011; Malagnini *et al.*, 2012; Massa *et al.*, 2013) (A to E in Fig. 4) and a velocity model (F in Fig. 4) derived in this paper from the geological interpretation and depth-conversion of the seismic line App. Orient. 1 (ViDEPI Project, 2014) along the trace of section B in Fig. 7b. In the location procedure, we assigned the standard WEIGHT OPTION coherently with the P and S weighting scheme and considered the option RELOCATE, in order to associate the time delays to seismic stations possibly affected by local velocity anomalies. We estimated the quality of the final locations, obtained from the six velocity models, accounting for the distribution of residuals of P- and S- phases (Res P, Res S), root mean square of travel-time residuals (RMS)

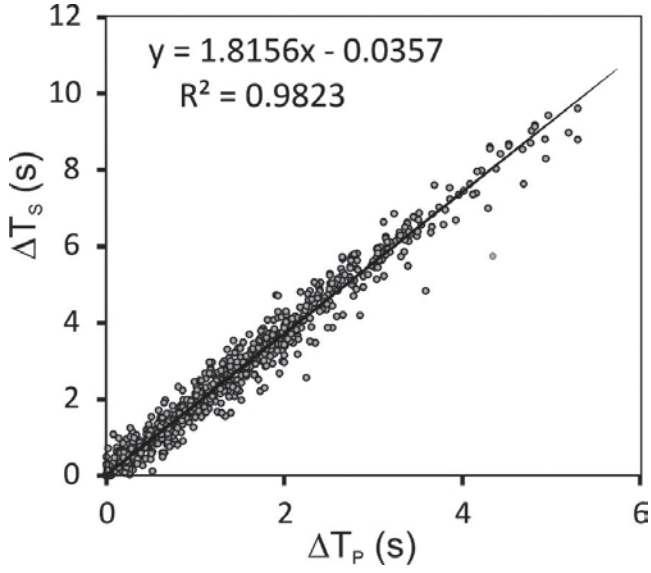

Fig. 3 - Modified Wadati plot; the data set consists of 546 P- and 244 S-phase arrival times associated with 41 selected earthquakes of the Emilia 2012 sequence (max M_W 6.1). The black line represents a simple least squares regression.

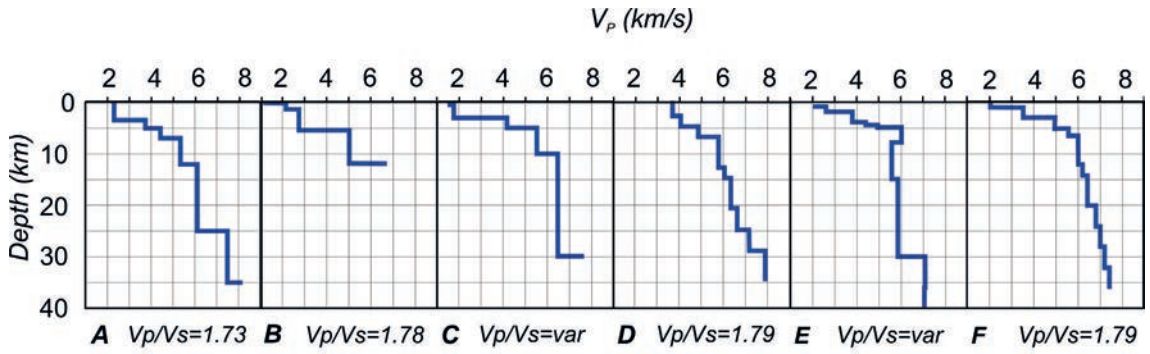

Fig. 4 - P velocity profiles of the models used to locate the major events (M_L ≥4.0) of the Emilia seismic sequence. Key: A = Costa *et al*. (1992), B = Zollo *et al*. (1995), C = Bragato *et al*. (2011), D = Massa *et al*. (2013), E = Malagnini *et al*. (2012), F = this study; var = variable.

and both horizontal and vertical formal errors (Err H, Err Z). The summary of these results in terms of Res P, Res S, RMS, Err H, and Err Z are shown in Fig. 5. The analysis of such location parameters is synthesized in Fig. 6, where the mean values of Res P, Res S, RMS, and the mean values of horizontal (Err H) and vertical errors (Err Z) are plotted and compared. The differences in terms of mean residuals (Res P, Res S, RMS) did not allow us to assess the quality of the seismic locations with respect to the six velocity models A-F (Fig. 6a). On the contrary, the distribution of the vertical formal errors differs according to the velocity model (Fig. 6b). Based on Fig. 6, we selected the velocity models named A, D, and F in Fig. 4 as the best ones among those analyzed. The corresponding epicentral distributions are reported in the map of Fig. 7a; the range of the hypocentral depth variation for each event is represented in the sections

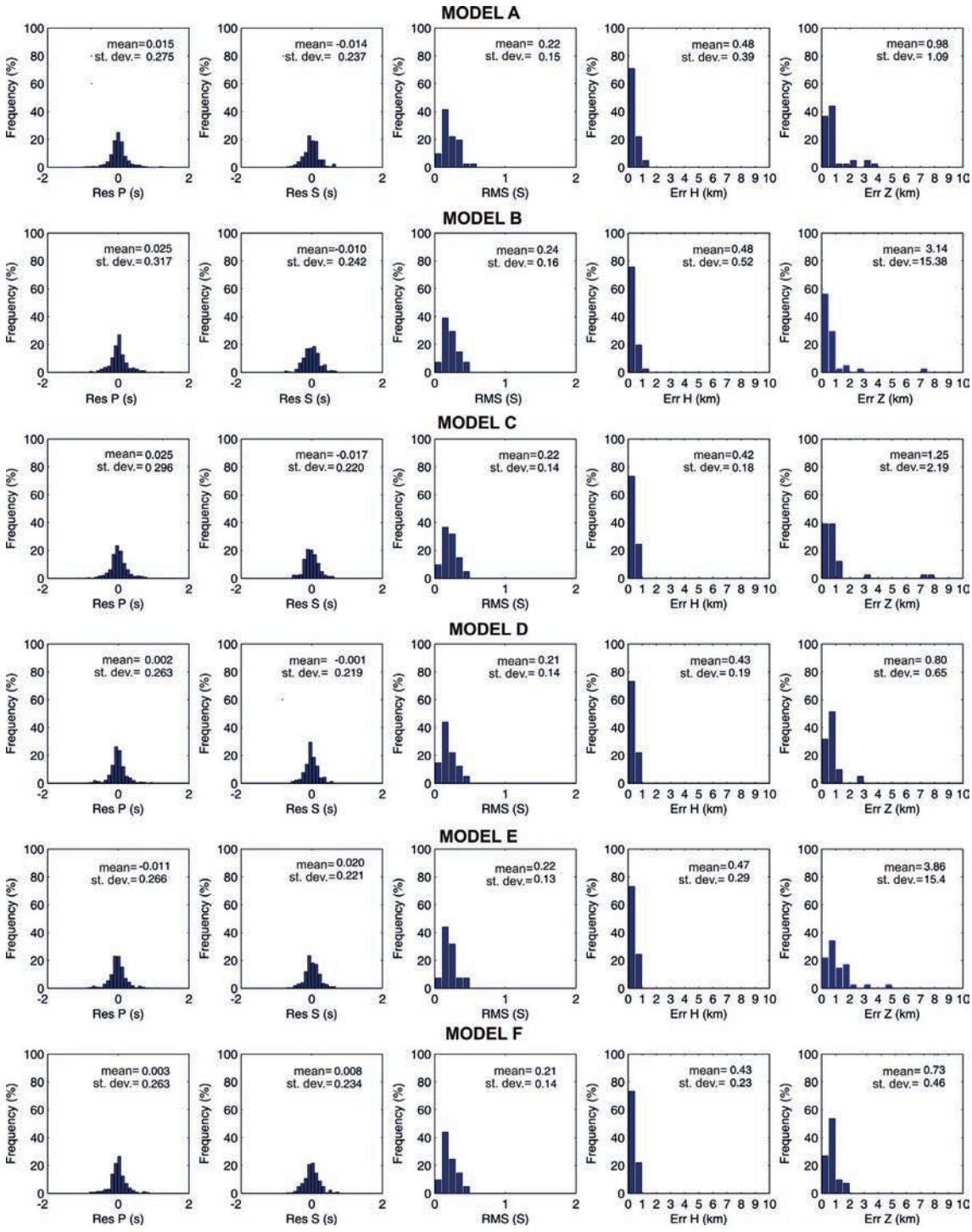

Fig. 5 - Summary of the results for the relocated events using P-wave velocity model from A to F. Histograms of absolute residuals of P- and S-phases (Res P, Res S); root mean square of travel time residuals (RMS); horizontal and vertical location formal errors (Err H, Err Z).

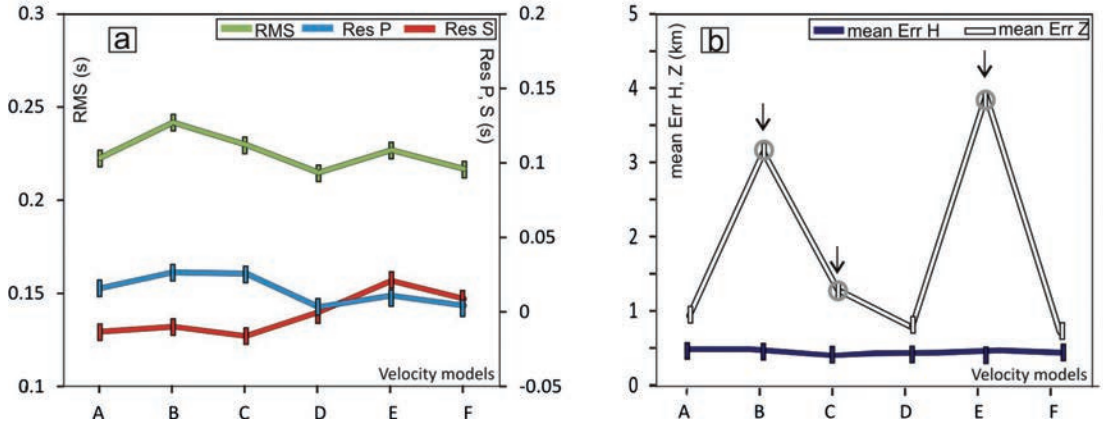

Fig. 6 - Analysis of location parameters: a) average RMS (green line), mean absolute P-phase residuals (light blue line) and mean absolute S-phase residuals (red line) for each studied velocity models; b) mean horizontal location errors (blue line) and mean vertical location errors (white line).

of Figs. 7b and 8 with a vertical bar, representing the standard deviation among the three best selected models. The hypocentral coordinates calculated for the three different velocity models are given in Table 1.

5. Emilia 2012 seismotectonic interpretation

5.1. Earthquake/fault association

To analyze the depth distribution of the relocated events (Table 1) with respect to the geometry of the Quaternary fold-and-thrust structures in the area, we projected the vertical bars corresponding to the standard deviation of the Emilia 2012 hypocentres derived from the selected velocity models, along the traces of two, independently and *a priori*, interpreted geological sections (sections A and B in Fig. 7b).

Section A extends across the May 29 epicentral area and coincides with the trace of a nearly N-S geological section across the Cavone field, initially interpreted by Nardon *et al*. (1990). The section clearly shows the Cavone fold structure, which involves the Meso-Cenozoic sequence from the Jurassic-Cretaceous shallow-to-deep water carbonates to the Upper Triassic Dolomia Principale Fm. The anticline is box-shaped with the forelimb overturned and displaced by high-angle thrusts, located at a depth of 4-5 km beneath the anticline crest. The high-angle thrusts splay at depths of 6-7 km from the underlying south-dipping low-angle Mirandola thrust, which also penetrates the Upper Triassic Dolomia Principale Fm, the Triassic evaporites, and the Lower Triassic-Permian meta-sediments (e.g., sedimentary basement). Because the section extends across the most arcuate portion of the Mirandola thrust, and in order to avoid spatial distortion, only the events belonging to the May 29 sequence (time interval from May 29 to June 12, 2012) located within a half-width of 6.5 km from the trace of the section were projected.

Section B was drawn along the trace of a seismic section ("App. Orient 1"), which extends in the NNE-SSW direction across the Ferrara Arc and the Emilia 2012 epicentral area (ViDEPI

Project, 2014). The seismic line was reinterpreted and depth-converted (Fig. 7b); the legend of the identified horizons is given in Fig. 7b. In section B, we clearly recognize, differing in this from other interpretations (Massoli *et al*., 2006; Toscani *et al*., 2009; Bertello *et al*., 2010; Bonini *et al*., 2014), five well distinct thrust segments. The innermost segment belongs to the MTS; the other four are splays of the FTS. All four FTS segments are blind faults that penetrate across the Mesozoic carbonate multilayer, reaching and cross-cutting the Triassic evaporites and the underlying sedimentary basement. In section view, they follow near-parallel down-dip trajectories, but in map view the segmentation pattern appears more complex (Fig. 7a). Also taking into consideration the FTS fold-and-thrust geometry, as schematically derived from the Structural Model of Italy in Fig. 1b (CNR - P.F. Geodinamica, 1990), four major near-parallel alignments may be identified (Fig. 7a). From south to north, they are named here: 1) Quarantoli, 2) Poggio Rusco-Casaglia, 3) Pilastri and 4) Sermide. Quarantoli and Sermide correspond to the Inner and Outer Ferrara thrusts of Fig. 1 (e.g., Internal and External thrusts *Auctorum)*, respectively. Poggio Rusco-Casaglia and Pilastri represent along-strike and perpendicular-to-strike segmentations of the Middle Ferrara Thrust, respectively.

In order to analyze the spatial relationships between the above segments and the Emilia 2012 seismic sequence, as a first approximation, we considered it acceptable to project along the trace of section B the overall relocated hypocentral data set (red and blue vertical bars in Fig. 7b), assuming a cylindrical deformation at a regional scale. This oversimplification has the advantage of offering a complete view of the earthquake/fault association. Subsequently, assuming a uniform half-width of 4 km, we projected the vertical bars along the traces of six interpretative sections (Figs. 8 and 9a). These sections were built across the epicentral area, taking into account the near-surface geometry and segmentation pattern of the major buried thrust fronts (Fig. 7a), the structural style of the fold-and-thrust structures as reconstructed in Fig. 7b, the available information from some hydrocarbon deep wells cutting across the Mirandola thrust (Cavone 1, Bignardi 1, Concordia 1 and Spada 1 wells), and the Casaglia segment of the Middle Ferrara Thrust (Casaglia 1 well) (data from ViDEPI Project, 2014), as well as the depth distribution of the relocated events.

Based on the reconstructed geometric earthquake/fault pattern (Fig. 8), integrated with information from the literature, we fix the following points, which can be significant for the characterization of the individual sources, as well as for the discussion of the likelihood of a triggered component in the Emilia 2012 earthquake sequence.

1 - The Emilia 2012 sequence, which began on May 20 and was preceded by a foreshock

Fig. 7 - Earthquake/fault association for the Emilia 2012 sequence: a) epicentral distribution of the events in the time interval from May 20 to June 12, 2012, as located in this paper according to the three best velocity models (A, D and F) discussed in the text (Table 1). Full symbols represent the events that occurred from May 20 to 28 and the empty ones the events that occurred from May 29 to June 12; the Sermide event that occurred on July 17, 2011, is also reported. Black lines are the traces of the two interpretative sections A and B. The blue and grey dashed line refers to the buried thrust fronts of the FTS segments and of the Mirandola Thrust, respectively; b) hypocentral view of the Emilia 2012 sequence as located in this paper, projected along the traces of two interpretative sections (Section A and Section B); the vertical bars represent the standard deviation of the selected solutions related to the three best velocity models (Table 1). Section A is from Nardon *et al*. (1990), slightly modified; the half width of the projected seismicity along the section is 6.5 km. Section B is derived from our interpretation of seismic line "App. Orient 1", available at ViDEPI Project (2014); the overall relocated Emilia 2012 data set (Table 1) is projected along the section trace. EQ1 and EQ2 are the main events (May 20 M_W 6.1 and May 29 M_W 5.8, respectively); EQ# is a May 29 event (11.00.01 UTC, M_W 4.4, event n. 30 in Table 1) located close to the Mirandola thrust plane.

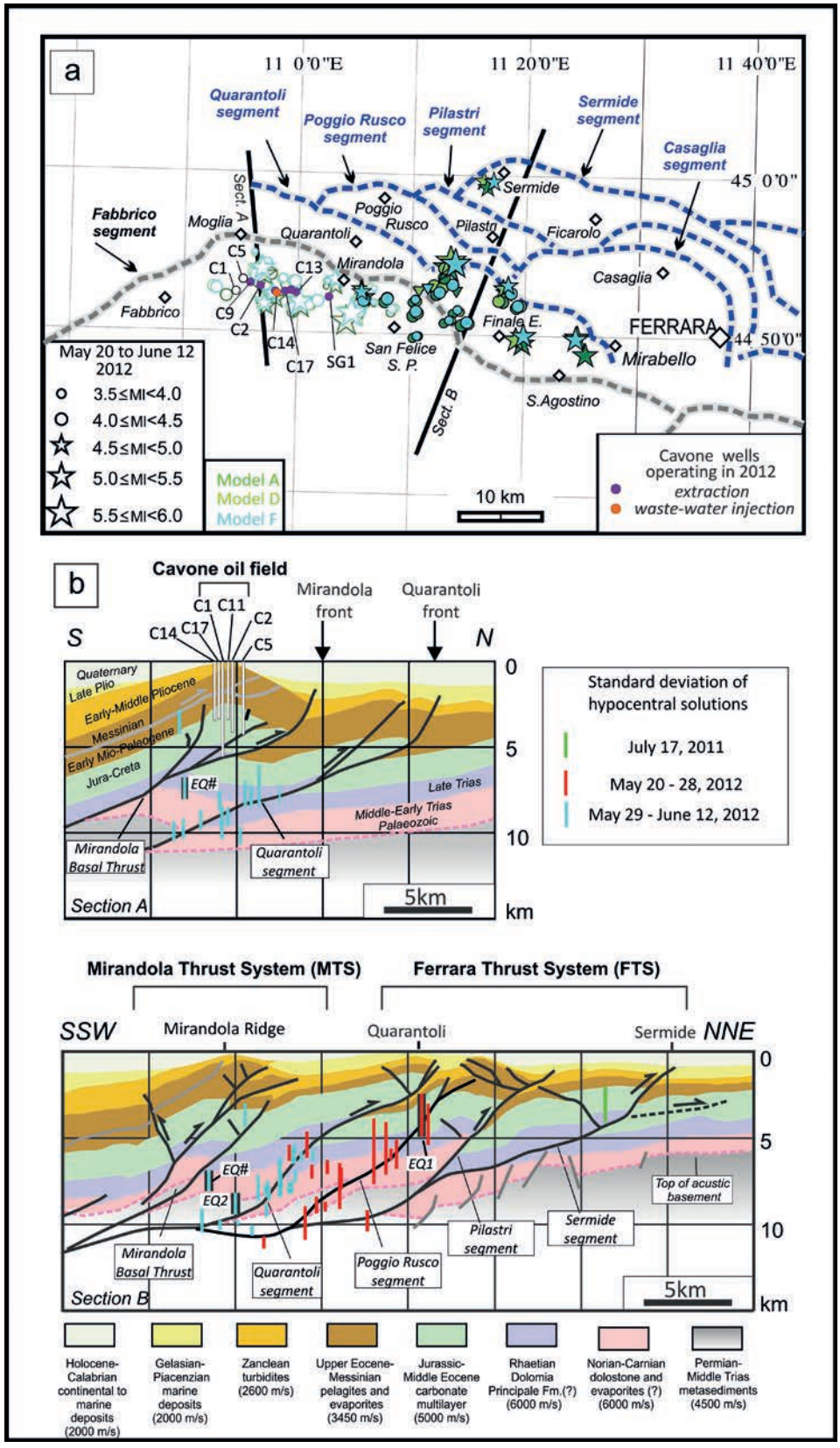
a
11 0'0"E
11 20'0"E
11 40'0"E
45 0'0"
44 50'0"
Quarantoli segment
Poggio Rusco segment
Pilastri segment
Sermide segment
Casaglia segment
Fabbrico segment
Sect. A
Sect. B
Moglia
Quarantoli
Poggio Rusco
Pilastri
Sermide
Ficarolo
Casaglia
Mirandola
Fabbrico
Finale E.
FERRARA
Mirabello
San Felice S. P.
S.Agostino
C1
C2
C5
C9
C13
C14
C17
SG1
May 20 to June 12 2012
3.5≤MI<4.0
4.0≤MI<4.5
4.5≤MI<5.0
5.0≤MI<5.5
5.5≤MI<6.0
Model A
Model D
Model F
10 km
Cavone wells operating in 2012
extraction
waste-water injection
b
Cavone oil field
C1 C11
C2
C5
C14 C17
Mirandola front
Quarantoli front
S
N
Quaternary
Late Plio
Early-Middle Pliocene
Messinian
Early Mio-Paleogene
Jura-Creta
EQ#
Late Trias
Middle-Early Trias Palaeozoic
Mirandola Basal Thrust
Quarantoli segment
Section A
5km
km
0
5
10
Standard deviation of hypocentral solutions
July 17, 2011
May 20 - 28, 2012
May 29 - June 12, 2012
Mirandola Thrust System (MTS)
Ferrara Thrust System (FTS)
SSW
Mirandola Ridge
Quarantoli
Sermide
NNE
EQ#
EQ2
EQ1
Top of acustic basement
Pilastri segment
Sermide segment
Mirandola Basal Thrust
Quarantoli segment
Poggio Rusco segment
Section B
5km
km
0
5
10
Holocene-Calabrian continental to marine deposits (2000 m/s)
Gelasian-Piacenzian marine deposits (2000 m/s)
Zanclean turbidites (2600 m/s)
Upper Eocene-Messinian pelagites and evaporites (3450 m/s)
Jurassic-Middle Eocene carbonate multilayer (5000 m/s)
Rhaetian Dolomia Principale Fm.(?) (6000 m/s)
Norian-Carnian dolostone and evaporites (?) (6000 m/s)
Permian-Middle Trias metasediments (4500 m/s)

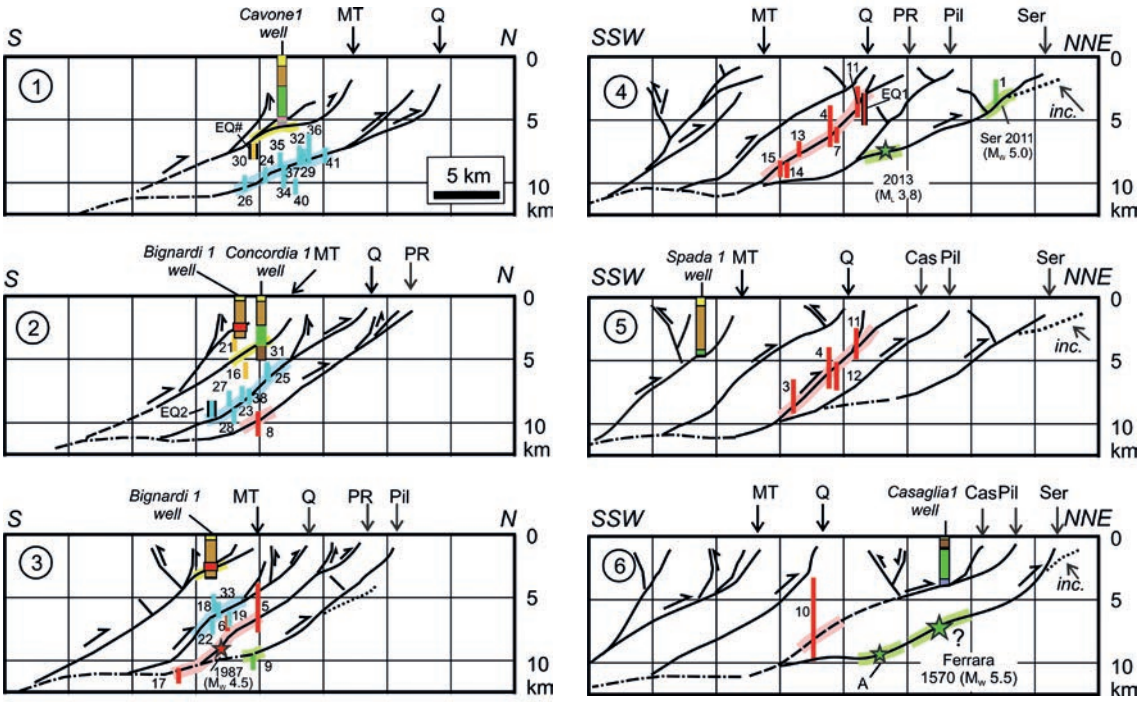

Fig. 8 - Earthquake/fault association for the Emilia 2012 sequence along the trace of interpretative serial cross-sections (traces of the sections in Fig. 9a). Sections 1 and 4 coincide with geological sections A and B in Fig. 7; in the other sections, the depth geometry of the thrust structures is interpreted taking into account the near surface tip-lines of the major buried thrust fronts as in Fig. 7a, the structural style of the fold-and-thrust structures as in Fig. 7b, the available information from hydrocarbon deep wells crossing the thrust segments and the relocated earthquake distribution (from Table 1). The stratigraphic layering drilled by the Bignardi 1, Cavone 1, Casaglia 1, Concordia 1, and Spada 1 wells (data from ViDEPI Project, 2014) is schematically represented with different colors (yellow = Plio-Quaternary, red = intra-Miocene thrust zones, brown = Late Eocene-Messinian, green = Jurassic-Early Eocene, pink = Late Triassic). Key for fault segments denomination: MT = Mirandola, Q = Quarantoli, PR = Poggio Rusco, Cas = Casaglia, Pil = Pilastri, Ser = Sermide, inc = incipient thrust. The colored vertical bars are the standard depth deviation for the Emilia 2012 events, as derived from Table 1; numbers from 2 to 20 refer to the May 20-28 time interval and numbers from 21 to 41 to the May 29 - June 12 time interval. The different colors of the bars represent the proposed attribution to the different fault segments; also, the colored strips along the fault traces highlight inferred seismogenic fault patches activated during the Emilia 2012 sequence and/or associated to other relevant earthquakes (light blue = Quarantoli, pink = Poggio Rusco and Casaglia, green = Sermide); the yellow strip in sections 1 and 2 highlights the subsidiary activation of the Mirandola thrust. The stars represent the approximate location of other events possibly associated to the here identified sources; star A represents the most external relevant event of the Emilia 2012 sequence (2012/05/20, 02:35, M_W 4.4), as relocated by Chiarabba *et al.* (2015). The 1570 Ferrara event has been tentatively attributed to the Sermide segment, based on the surface location of the corresponding box-shaped source as given by Pettenati *et al.* (2013) and Vannoli *et al.* (2014).

(M_W 4.1) on May 19, progressively activated different segments of the FTS (Fig. 7b). The first large event, e.g., EQ1 (M_W 6.1), nucleated on the Poggio Rusco segment (Figs. 7b and 9b), at a depth of about 4 km (Table 1), close to the vertical transition between the Jurassic carbonates and the underlying Upper Triassic dolostones (Fig. 7b). The rupture propagated down-dip with an eastward directivity (Convertito *et al.*, 2013). The EQ1 aftershock sequence (May 20 to 28) grew bilaterally from the main event in an average WNW-ESE direction (Fig. 1c). It covered an epicentral area extending for about 25 km along the Poggio Rusco segment and for about 10 km along the Casaglia segment (Figs. 1c and 9c). Along-dip, the May 20-28 hypocentral volume was confined within the highly competent Upper Triassic layers, at depths between 4 and 9 km

(Fig. 7b). The second large event, e.g., EQ2 (M_W 5.8), nucleated nearly 15 km WSW-wards from EQ1, at a depth of about 8.5-9.0 km (Table 1), activating the Quarantoli segment. According to the interpretation proposed in Fig. 7b, the EQ2 hypocentre was located close to the transition between the Rhaetian dolostones (Dolomia Principale Fm.?) and the underlying Norian-Carnian evaporites (Burano Fm?). The rupture propagated quasi-bilaterally with a dominant westward directivity (Convertito *et al*., 2013). The May 29 - June 12 EQ2 aftershock sequence (Fig. 7a) extended prevailingly in the E-W direction, for a length of about 25 km. The western termination of the Emilia 2012 sequence coincided with the WSW-ENE trending left-lateral ramp of the Mirandola Arc (Govoni *et al*., 2014). Along-dip, the May 29 to June 12 hypocentral volume was confined within the highly competent Upper Triassic sedimentary sequence, at prevailing depths between 5 and 10 km (Fig. 7b).

2 - The hypocentres, projected in the sections of Figs. 7b and 8 as depth interval bars, show that the May 20 to 28 aftershock sequence (red bars in Fig. 7b) primarily activated the Poggio Rusco segment, at depths between 3-4 to 9-10 km, delineating a seismogenic patch dipping in average 35° southwards, with locally steeper dip-angles (45°-50°) (see sections 3, 4 and 5 in Fig. 8). A few events of the same aftershock group subordinately illuminated the lower flat of the Poggio Rusco segment at depths of about 11 km (event n. 17 in Table 1), as well as the lower flat of the Sermide segment at depths of about 10 km (e.g., event n. 9 in section 3 of Fig. 8). The May 29 to June 12 aftershock sequence (blue bars in Fig. 7b) activated primarily the Quarantoli segment, at depths between 6-7 and 10-11 km, delineating a seismogenic patch dipping in average from 20° to 35° SSW-wards (see sections 1, 2, and 3 of Fig. 8). Few May 29 events (Eqs. n. 16, 21, and 30 in Table 1) fall outside this prevailing seismogenic volume and appear located in the surroundings of the Mirandola thrust.

3 - The depth distribution of the more energetic events of the Emilia 2012 sequence, as relocated in this paper (Figs. 7b and 8), highlights an average moderate dip-angle of about 30°-35° for both the EQ1 and the EQ2 fault sources. Conversely, Govoni *et al*. (2014), based on a relocated earthquake catalogue of the overall sequence, estimate for the EQ2 fault a high-angle dip of about 70°. Also, considering that the available focal solutions of the May 29 event and those of its aftershocks show moderate to small south-dipping angles [RCMT by Pondrelli *et al*. (2012); TDMT by Scognamiglio *et al*. (2012)], we argue that the steep aftershock volume, which is mainly confined at depths between 4 and 7 km [section B-B1 in Fig. 6b in Govoni *et al*. (2014)], does not represent the main event fault source, but rather a high-angle splay activated by the microseismic activity. Our data set shows, as well, that the Emilia 2012 more energetic events are all confined within the hanging-wall rock volume of the Ferrara Basal Thrust, at depths shallower than 10-11 km. Therefore, we tend to exclude the activation by the main events of any steep-dipping fault segment in the footwall of the Mirandola frontal thrust, as suggested by other authors (Govoni *et al*., 2014; ICHESE, 2014).

5.2. Characterization of the individual seismogenic sources

According to our reconstruction and interpretation, the Emilia 2012 sequence and the previous neighbouring 2011 seismicity activated a rather complex pattern of along-dip and along-strike interconnected fault segments, all belonging to the FTS. The two major events, EQ1 and EQ2, nucleated on the Poggio Rusco and Quarantoli left-lateral *en echelon* segments, respectively, but the overall sequence also strongly involved the Casaglia segment, e.g., the

along-strike prosecution of the Poggio Rusco segment (Fig. 7a). The July 2011 sequence activated the outermost Sermide FTS splay. By schematizing the buried traces of the identified FTS segments, as derived from the Structural Model of Italy (CNR - P.F. Geodinamica, 1990), and connecting points of equal depth along their down-dip trajectory, as interpreted in the serial cross-sections of Fig. 8, we schematically draw the depth contour lines of each fault segments. As all seismogenic master faults, these segments, which were only partially activated during the Emilia 2012 sequence, are intended as irregular surfaces of finite extent. Their upper border simply coincides with the buried near-surface cut-off line. Their lower border corresponds to a branch line located at the intersection of the considered segment with an innermost segment or with the basal detachment, as interpreted in the sections of Fig. 8. Their lateral borders correspond to a tip line, in the case of *en echelon* segments (e.g., Quarantoli), or to the intersection line between two along-strike nearly continuous segments, as in the cases of Poggio Rusco and Casaglia.

The reconstructed isobath map in Fig. 9b shows the shape, size, and the spatial relationships among the identified FTS fault segments. On the same map, the major historical and instrumental earthquakes tentatively associated with the different sources are reported. The preferential seismic planes derived from the available focal solutions are also drawn; they all dip at low-angle southwards with strongly prevailing dip-slip reverse kinematics. The average fault parameters in terms of strike, dip, length, surface width (the latter measured between the buried fault trace and the horizontal projection of fault branch-line at depth), and depth are given in Table 2. An average rake angle is also indicated; it has been evaluated assuming an average direction of regional transport at the front of the Padan Arc oriented about N15°±5°, as indicated by strain axes from geodetic data, Sh_{max} from borehole breakouts and slip vectors on preferential seismic planes from focal mechanisms (Devoti *et al.*, 2011; Montone *et al.*, 2012). In Table 2, the slip rate values from Vannoli *et al.* (2014) and the most significant historical and instrumental earthquakes possibly associated with the sources (Fig. 9a) are also reported.

The Quarantoli segment extends for ~25 km in a N100°E average direction, with an average surface width of ~15 km and with an average inclination of ~35° from near surface to a depth of ~11 km. Four of the Emilia 2012 events with M_L and/or M_W >5.0 (ns. 20, 28, 29, and 36 in Table 1) may be associated with this source. Three of these events occurred on May 29 (among which the main M_W 5.8 event, e.g., EQ2), and one on June 3. The preferential seismic planes derived from available focal solutions dip at low-angle southwards with strongly prevailing dip-slip reverse kinematics and a very subordinate left-lateral component (rake 85°). No historical earthquake from the CPTI11 catalogue may be associated with this source, but the macroseismic epicentre of two recently discovered historical events [Mirandola 1761 and Moglia 1778: Castelli *et al.* (2012)] fall within its surface boundaries.

The Poggio Rusco segment extends for ~25 km in a N105°E average direction, with an average surface width of ~16 km, with an average inclination of ~30° from near surface to a depth of ~10 km and with almost pure dip-slip kinematics (rake 90°). The strongest event of the Emilia 2012 sequence (e.g., EQ1, M_W 6.1, depth ~4 km) may be associated with this source, together with another relevant May 20 event (n. 8 in Table 1) occurred nearly one hour after EQ1, at a depth of about 10 km, nearly 10 km SW-wards of EQ1. The 1987 Bassa Modenese south-dipping thrust event (M_W 4.6), reported in Carminati *et al.* (2010), and the historical 1901 Poggio Rusco event (M_W 4.7) might be tentatively associated with this source (Fig. 9b).

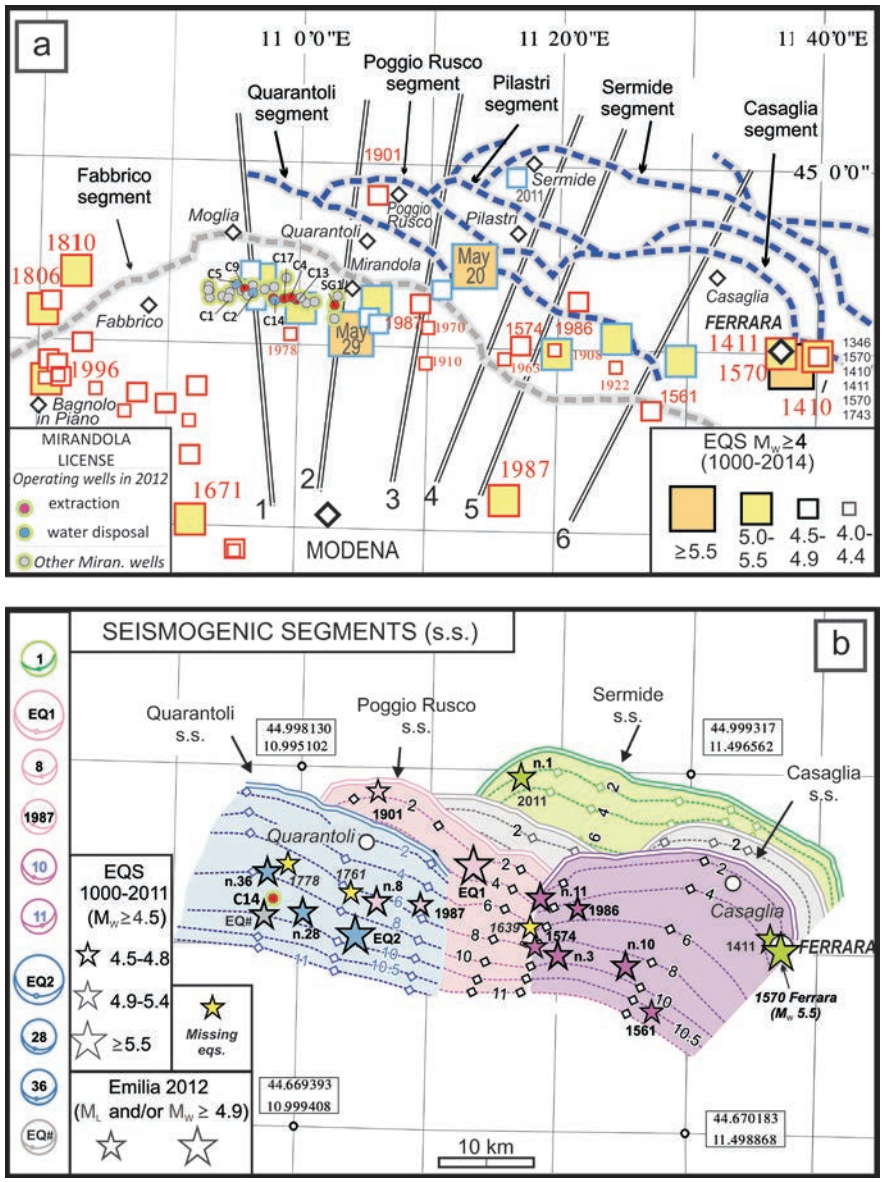

Fig. 9 - Seismotectonic interpretation of the Ferrara Thrust System (FTS) with reconstruction of the individual seismogenic segments partially activated during the Emilia 2012 sequence: a) major earthquakes (M_W≥4.0) from the CPTI11 database (Rovida *et al*., 2011) (red outlined squares) and from the relocated Emilia 2012 sequence (blue outlined squares). Black and white lines are the traces of the sections reported in Fig. 8. b) Surface projection (colored areas) and depth contour lines (dashed lines) of the FTS seismogenic faults, as reconstructed in this paper, based on the interpolation of depth points (small white diamonds) measured along the down-dip traces of the seismogenic segments drawn in the interpretative sections of Fig. 8. Color key for the seismogenic sources: light blue = Quarantoli, pink = Poggio Rusco, light purple = Casaglia, grey = Pilastri and its eastern along-strike prolongation, green = Sermide. The stars represent the major Emilia 2012 events (M_W and/or M_L ≥4.9) plus the historical and instrumental earthquakes from 1000 to 2011 with M_W≥4.5, falling within the boundaries of the sources; the different coloured stars highlights the inferred source attribution, as discussed in the text. EQ1, EQ2, and EQ# as in the caption of Fig. 7. The yellow dots represent the macroseismic epicentres of events missing in the CPT11 catalogue and highlighted by Castelli *et al*. (2012). The column on the left presents the preferential seismic planes for the major Emilia 2012 events, derived from the focal solution given by Saraò and Peruzza (2012); the number inside the focal sphere and on the map refers to the earthquake number in Table 1; the focal mechanism for event 1987 (Bassa Modenese, M_W 4.6) is from Carminati and Vadacca (2010). The map is projected using a Lambert Conformal Conic projection (13.0, 42.0, 39.0 and 45.0 are central meridian, latitude of origin, and standard parallels, respectively; GCS:WGS84).

Table 2 - Geometric and kinematic parameters of the individual fault segments involved in the Emilia 2012 thrust sequence as interpreted in Figs. 7b and 8 and reconstructed in Fig. 9. Both along-strike and along-dip, the identified fault segments are non-planar, irregular, surfaces; therefore, the fault parameters given in this table represent average schematic values, obtained from more detailed values measured at different depths and location. The depth value, H, refers to the bottom fault boundary, located at the intersection line (e.g., branch line) of the considered segment with an innermost segment or with the basal detachment. The rake angle is evaluated assuming an average direction of regional transport at the front of the Padan Arc oriented about N15°±5°, as indicated by strain-rate axes from geodetic data, sh-max from borehole breakouts. and slip vectors on preferential seismic planes from focal mechanisms (Devoti *et al.*, 2011; Montone *et al.*, 2012). Slip rate values are from Vannoli *et al.* (2014). The major Emilia 2012 events and, tentatively, the historical earthquakes (from Rovida *et al.*, 2011, and from Castelli *et al.*, 2012, for the events with asterisks) are assigned to the various fault segments.

Ferrara Thrust System (FTS)		Individual segments average parameters			Emilia 2012 major earthquakes (as in Tab.1) (MW or ML ≥ 4.9) plus Sermide event 2011					Major earthquakes in the region from 1000 to 2011 (MW ≥ 4.5)			
First-order alignments	Individual segments	Attitude S=Strike D=Dip angle R=Rake	Dimension (km) L=Length Ws=Surf. Width H=Depth	Slip rate (cm/y)	n. in Tab.1	Date	ML	MW	Depth (H)	Locality	Date	Io MCS	MW
Inner Ferrara Thrust	Quarantoli	S=N100°±5° D=35°±10° R~85°	L=25±1 Ws=15±1 H =10.5±0.5	0.25-0.50	20-EQ2 28 2 36	May 29 May 29 May 29 June 3	5.8 5.3 5.2 5.1	5.8 5.5 - 5.1	8.6-8.8 9.7-9.9 7.1-8.3 5.1-5.8	*Mirandola** *Moglia**	1761 1778		
Middle Ferrara Thrust	Poggio Rusco	S=N105°±5° D=30°±10° R~ 90°	L=24±1 Ws = 16±1 H= 9.5±0.5	0.10-0.50	2-EQ1 8	May20 May20	5.9 4.9	6.1 5.3	2.9-5.3 9.2-10.9	Poggio Rusco Bassa Modenese	1901 1987	6 6	4.7 4.6
	Casaglia	S=N115°±5° with lateral bends D= 30°±10° R~100°	L=23±1 Ws=17±1 H=9.5±0.5	0.10-0.50	3 10 11	May 20 May 20 May 20	5.1 5.1 4.5	4.5 5.3 4.9	6.1-8.6 3.2-10.8 3.1-5.0	Finale Emilia *F.Emilia-Carpi ** Bondeno	1574 1639 1986	6 7-8 6	4.7 - - 4.7
Outer Ferrara Thrust	Sermide	S=N110°±5° with lateral bends D=25°±10° R~95°	L=32±2 Ws=18±2 H=8.5±1.5	0.10-0.50	1	July 17 2011		5.0		Ferrara Ferrara Ferrara Ferrara Ferrara	1346 1410 1411 1561 1570	6-7 6-7 7 5-6 7-8	4.9 4.9 5.1 4.5 5.5

The Casaglia segment extends for ~23 km in a N115°E average direction, with an average surface width of ~17 km and with an average inclination of ~30° from near surface to a depth of ~10 km. Again, the preferential seismic plane derived from available focal solutions dip at low-angle southwards with prevailing dip-slip reverse kinematics and a very subordinate right-lateral component (rake 100°). Three of the major Emilia 2012 events (M_W or M_L ≥4.9), which occurred on May 20, may be associated with this source (ns. 3, 10, and 11 in Table 1). The macroseismic epicentres of a few historical events, with M_W between 4.0 and 5.0, are located within the boundary of this source, as depicted in Fig. 9b, mainly close to the lateral transition with the Poggio Rusco source, in the localities of Finale Emilia (1574, M_W 4.7; 1908, M_W 4.3), Bondeno (1986, M_W 4.6) (Fig. 9) and Finale Emilia-Carpi (April 6, 1639, maximum intensity VII-VIII MCS) (Table 2 and references therein). The macroseimic epicentres of some historical Ferrara earthquakes, as the 1411 (M_W 5.1) and 1570 (M_W 5.5) events, fall at the eastern boundary of this source, but, evidently, they do not necessarily belong to this source.

The Sermide segment extends for ~32 km in a N110°E average direction, with an average surface width of ~18 km and an average inclination of ~25° from near surface to an average depth of ~8.5 km. This source was not deeply involved in the Emilia 2012 sequence, but was

activated by the Sermide 2011 earthquake (M_W 5, event n. 1 in Table 1). This event is sited 15 km NNE-ward of EQ1 at a depth of 3-4 km (Fig. 7b). It presents a thrust focal mechanism with a south-dipping preferential seismic plane and a N-S trending P-axis (Fig. 1c), similar to those of the Emilia 2012 events (Fig. 1c). In light of the map-view location of the box-shaped 1570 individual source, as given in the literature (Pettenati *et al.*, 2013; Vannoli *et al.*, 2014), the hypothesis of an association of the 1570 earthquake with the Sermide source may be advanced (see section 6 of Fig. 8).

Summarizing, the reconstructed FTS fault segments are all substantially similar in size (about 25 km long and 15-18 km wide), apart from the slightly larger Sermide segment, and in the average dip-angle (25° to 35°). A variation in strike from nearly E-W to nearly WNW-ENE is evident going from the Quarantoli source towards the Casaglia one. This pattern is well supported by the attitude of the major events' preferential seismic planes (Pondrelli *et al.*, 2012; Scognamiglio *et al.*, 2012), as well as by the elongation axes of the co-seismic *en echelon* ground doming revealed by InSAR data (Tizzani *et al.*, 2013).

5.3. Some further hints

1 - The Emilia 2012 seismogenic fault patches, highlighted by the hypocentral distribution, ruptured along-strike throughout almost the entire Quarantoli and Poggio Rusco segments (for a total length of about 35 km), plus a large portion of the Casaglia segment (for an additional length of about 15 km). As in other such cases around the world, the segmentation pattern appears to control the nucleation and the extent of earthquake ruptures (Manighetti *et al.*, 2015). Therefore, the identified segmentation pattern may help to explain the unusual large size of the Emilia 2012 epicentral area, which as a whole extends for about 50 km along strike (Fig. 1c), with a length far beyond the rupture length derived from scale laws. In fact, if we exclude the seismic activity associated with the independent Casaglia segment, the along-strike length of the Quarantoli and Poggio Rusco segments is closer, although still great, to the subsurface rupture length yielded for EQ1 (M_W 6.1) and EQ2 (M_W 5.8) by the Wells and Coppersmith (1994) relationships.

2 - Based on the long-term kinematic/geometric evolution of the Ferrara Arc, as reconstructed on the basis of stratigraphic-structural constraints (Ghielmi *et al.*, 2010) and on the present deformation field, as derived from geodetic and earthquake data, we consider that in Middle Pleistocene times (at about 0.6 My), the Ferrara Arc had almost achieved its present geometric configuration. Since then, the active NNE-directed compression was mainly localized along the frontal sectors of the arc, e.g., the WNW-ESE striking FTS, and the WSW-ENE lateral ramp of the MTS. Conversely, the WNW-ESE striking frontal portion of the Mirandola Thrust was abandoned and not active anymore. In such a context, the observed uplift of the Cavone anticline that occurred in the Late Pleistocene and Holocene (0.16 mm/yr, Scrocca *et al.*, 2007) would not represent active Mirandola thrusting, but might be related to the displacement occurred on the innermost FTS segment (e.g., Quarantoli segment), passively carrying the pre-existing Mirandola compressional structure.

3 - The time-space distribution of the historical and instrumental events associated with the NNE-directed thrust process at the front of the Ferrara Arc shows how the seismogenic deformation progressively migrated westward along-strike, activating different *en echelon* segments. The 1570 earthquakes may have ruptured the easternmost FTS segment (e.g.,

Sermide in our reconstruction) (Fig. 8), whereas the Emilia 2012 sequence ruptured the two westernmost ones (Poggio Rusco and Quarantoli). A further westward migration of the rupture process might find a physical barrier played by the sharp change in direction of the front of the Ferrara Arc, which assumes an ENE-WSW strike along the lateral Mirandola ramp. We cannot exclude that in the future the earthquake rupture process might effectively jump from the S-dipping Quarantoli Thrust, activated by the May 29 event, to a lateral SSE-dipping structure (Fabbrico segment in Fig. 9a), thus continuing its westward propagation pattern.

6. Discussion on the likelihood of triggering effects

6.1. Models and results in the literature

The likelihood of triggered seismic activity in the Emilia 2012 thrust earthquakes due to hydrocarbon exploitation and related activities within the Cavone field was deeply explored by two international committees, Astiz *et al*. (2014) and ICHESE (2014). These two committees used geological, seismological, and geophysical data with statistical analyses and/or mechanical modelling. They reached different conclusions, both regarding the geometry and structural style of the activated fault system and the likelihood of triggered effects.

ICHESE (2014) interpreted the Ferrara Arc as a low-angle fault-bend-fold system developed in the hanging-wall of a first-order flat-and-ramp basal thrust. Specifically, the Mirandola thrust was interpreted as the portion of the basal thrust underlying the Cavone reservoir, and the Ferrara Thrust as one of the hanging-wall second-order breaches, splaying from the basal Thrust. The May 20 event was interpreted as being located at depths of ~5 km on the Ferrara Thrust and the May 29 at depths of ~9 km on a blind high-angle thrust, located beneath the Cavone reservoir within the Mirandola Thrust footwall volume. A completely different geometric interpretation was the one proposed by Astiz *et al*. (2014). These authors reconstructed a fault-propagation fold system organized in two independent first-order thrust structures, Mirandola and Ferrara, each articulated in high-angle fault segments (average dip angle of 45°-50° for Mirandola and 55°-60° for Ferrara) propagated to depths of 18-20 km. They located the May 29 event on the northern Mirandola segment at depths of about 5 km, and the May 20 event on the Middle Ferrara segment, at a depth of about 10 km.

ICHESE (2014) highlighted that the extraction/injection activities during the life of the Cavone reservoir determined a net depletion of the reservoir (negative volume difference of 21%) with a consequent negative static stress change that would have inhibited earthquake activity rather than enhancing it. On the other hand, they observed a statistical correlation of the last pre-May 20 seismic activity and the May 20 main event with pressure increase within the C14 wastewater injection well, a deep well (3350 m) of the Cavone field, active in the time period 2011-2012. Therefore, they advanced the hypothesis that fluid circulation from the reservoir might have reached the Ferrara Thrust, which in their interpretation was in physical and hydraulic connection with the Mirandola Thrust, perhaps triggering the May 20 earthquake. Conversely, they excluded triggering effects for the May 29 event, mainly because, in their interpretation, its source thrust was separated from the overlying Mirandola Thrust and Cavone reservoir by a thick layer of marly deposits, which would have constituted a real barrier for fluid circulation.

Astiz *et al*. (2014) rejected the hypothesis of fluid-injection-driven triggering in the May 20 case not only because they did not recognize any statistical correlation and calculated negligible values of stress changes, but also because in their geometric interpretation, the Mirandola and Ferrara thrusts were independent structures, not in contact. Based on physical-mathematical models and associated simulations, Astiz *et al*. (2014) calculated at the May 20 hypocentre a Coulomb stress variation close to zero due to fluid injection, extremely small stress increases (0.09 mbar) due to mass removal, and slightly negative variations (less than a mbar) due to pore-elastic stress changes. At the May 29 hypocentre, they calculated a negligible (<0.01 bar) Coulomb stress variation due to fluid injection, an extremely small increase (0.09 mbar) due to mass removal, and slightly negative variations (less than 1 mbar) due to pore-elastic stress changes. More significant Coulomb stress variations (up to 2-3 bar) were calculated by Astiz *et al*. (2014) as a result of fluid injection within the C14 wastewater well (Fig. 2), but the modeled perturbation ring only extended a few hundred metres around the well and, therefore, it would not have been capable of reaching the May 20 and 29 hypocentral areas. Summarizing, according to Astiz *et al*. (2014), the evaluated stress changes are too small (<0.1 bar) and localized to be able to produce any effect (retarding or anticipating) on both the May 20 and 29 fracturing processes, also considering that a value of 6 bar was calculated for the static Coulomb stress triggered by the May 20 main event on the May 29 source (Pezzo *et al*., 2013).

6.2. Spatial interplay between seismogenic faults and extraction/injection wells in the Cavone oil field

From the above discussion it seems evident that an unloading-related triggered seismicity is unlikely in the Emilia 2012 sequence case, substantially due to the modest Cavone field size, the modest long-term extraction volumes (average yearly production during the last seven years was 30,000 tons) and, most of all, the lack of a net reservoir depletion. Conversely, fluid injection processes, such as those associated with the C14 wastewater disposal, might be responsible for significant Coulomb stress variations (up to 2-3 bar), but, according to the Astiz *et al*. (2014), the latter would have remained too localized around the well itself to be responsible for triggering effects on the two major events of the Emilia 2012 sequence.

In the more general literature on induced/triggered activity (Grasso, 1992; Grasso and Sornette, 1998; Mulargia and Bizzarri, 2014 among many others), it has been demonstrated that: 1) even very small overpressure (<1 bar) due to injection fluids may be capable of triggering destructive earthquakes (M >5.5) on a nearby active fault; 2) fluid may propagate as a slow stress wave for large distances (tens of kilometres); 3) destructive earthquakes (M >5.5) may also occur with large time delays (even 10 years) far from the injection site. Therefore, the knowledge of the deep fault pattern is crucial to identify the likelihood of fluid paths that might favour the connection between the reservoir and the hypocentral area. In order to identify the presence or not of suitable fluid paths in the Emilia 2012 specific case, as well as in the case of future earthquakes in the same area, we summarize the here reconstructed spatial relationships among the Emilia 2012 earthquakes, the Cavone oil field, and the identified seismogenic segments.

1 - The May 20 main event (EQ1, M_W 6.1) nucleated far from the Cavone oil field, at an epicentral distance of about 20 km ENE-wards of the injection well Cavone 14 (C14), at a depth of about 4 km (Figs. 2 and 7). The rupture did not propagate towards the oil field, but further

east (Convertito *et al*., 2013). The EQ1 aftershock sequence extended in a nearly WNW-ESE direction, entirely eastwards of the Cavone oil field (from about 10 to about 35 km eastwards of C14) (Fig. 7a). The EQ1 seismogenic thrust (e.g., Poggio Rusco segment) was not in any physical contact with the Cavone reservoir or with the underlying Mirandola Thrust. It was separated from both of them by the fold-and-thrust rock pile of its own hanging-wall and by that of the Quarantoli segment hanging-wall (see section B in Fig. 7b).

2 - The May 29 main event (EQ2, M_W 5.8) nucleated at a closer epicentral distance from the Cavone field (~10 km westwards of C14), at a depth of about 9 km. Its sequence extended in a nearly E-W direction, from about 8 km eastwards to about 15 km westwards of C14 (Fig. 7a). Although the EQ2 epicentral area largely overlapped with the Cavone oil field, there was no direct and/or indirect contact between the EQ2 seismogenic patch and the reservoir at the hypocentral depths. In fact, the EQ2 seismogenic patch is not a portion of the Mirandola thrust, underlying the Cavone anticline, but rather of the deeper Quarantoli segment (Fig. 7). According to our geometric interpretation (Fig. 7b), this segment does not show any physical contact with the Mirandola Thrust and is separated from it, and from the Cavone reservoir, by the its own hanging-wall rock volume.

3 - Four of the relevant EQ2 aftershocks (M_L or M_W ≥4.9 in Table 1) had their epicentres located just above the Cavone oil field, at horizontal distances less than ~3 km with respect to the C14 well (Fig. 2). In section view (Figs. 7b and 8), three of them (two dated May 29 and one June 3, ns. 28, 29 and 36 in Table 1) appear unrelated to the Mirandola Thrust and rather associated with the Quarantoli segment. Conversely, the fourth one (May 29 at 11.00.01 UTC, M_W 4.4, depth 7.5, n. 30 in Table 1), hereafter referred to as EQ#, is located close to the Mirandola Thrust, at a horizontal distance of ~2 km and a vertical distance of ~4 km from the C14 bottom (Fig. 7b). Close to the Mirandola Thrust, and beneath the Cavone reservoir, are also located two smaller events of our data set, one that occurred on May 25 (M_W 4.2, depth 5-6 km, n. 16 in Table 1) and the other on May 29 at 07.07.18 UTC (M_L 4.0, depth about 4 km, n. 21 in Table 1) (Fig. 8). We consider that these three events (e.g., ns. 16, 21, and 30 in Table 1), which are located far from the two main EQ1 and EQ2 seismogenic patches (Poggio Rusco and Quarantoli segments) and close to the Mirandola thrust and the C14 well, might indeed represent triggered events of the Emilia 2012 sequence due to fluid pressure increase at the C14 well.

4 - In correspondence with the Cavone epicentral area, the Emilia 2012 earthquake catalogue relocated by Govoni *et al*. (2014) shows: a) a relevant clustering of macroseismic activity (events up to M_L 3.5 plus a few ones with M_L 3.5-4.0) located at depths between 3.0 and 4.5 km; b) another distinct group of events (M_L up to 5.0, including our three previously discussed events ns. 16, 21, and 30) located at depths between 4.5-6.0 km; c) a third group of deeper events, including EQ2, located in the 7-9 km depth range. We observe that the shallow low-seismicity layer (3.0-4.5 km) is just concentrated at the Cavone hydrocarbon reservoir depths and that the intermediate-depth seismic layer (4.5-6.0 km) well coincides, in our interpretation (Fig. 8), with the portion of the Mirandola Thrust that underlies the oil field and that is not far from the region close to C14. Therefore, we advance the hypothesis that an increase of pore pressure immediately below the reservoir, stimulated by fluid injection and waste storage, might have favored such seismicity (triggered or even induced), moving the Mohr circle towards the origin and thus reactivating the now tectonically inactive frontal sector of the Mirandola Thrust.

Conversely, the deeper third group of events (7-9 km depth) beneath the Cavone oil field well coincides with the seismogenic patch of the Quarantoli segment, as interpreted in this paper (Figs. 7b and 8). Therefore, in our opinion, for this third group of events, a human-activity triggered component can be excluded.

5 - The C14 wastewater injection well, as several other wells of the Cavone field shown in the maps of Figs. 7 and 9, falls within the western half of the Quarantoli source, close to the northern end of the WSW-ENE striking left-lateral lateral segment of the MTS. Whereas the southern portion of this segment is associated with historical and instrumental activity (e.g., 1831 and 1832 M_W 5.5; 1806 and 1810 M_W 5.0-5.5; Reggio Emilia 1996 M_W 5.4), its northern portion, which extends for nearly 15 km from Fabbrico towards Moglia (Fabbrico segment in Fig. 9a), is not connected with any historical or present seismic activity. Therefore, the question arises whether a net injection pressure increase, such as that observed at C14 and localized close to the northern end of the Fabbrico segment, might favor the rupturing process, thus anticipating the occurrence of future strong earthquakes ($M_W \geq 5.5$).

7. Conclusions

In this paper, based on our earthquake relocation (M_W prevalently ≥4, Table 1) and geologic interpretation, we identify the fault segments involved in the Emilia 2012 sequence and define their geometry, structural style, and deep interplay. Our goals were: a) to propose an updated individual source model for the FTS and, b) to verify if the tectonic pattern was favorable to a possible propagation of injection-related fluids and pressure variations from the Cavone oil field to the seismogenic patches, with consequent implications in terms of triggered effects. The main results and/or points that warrant further discussion can be summarized as follows.

1 - The dominant structural style within the Emilia 2012 seismic area is that of a basement involved low-angle fault-propagation fold system, with two distinct major thrust systems, the Mirandola and Ferrara ones (MTS and FTS), splaying up from the common SSW-dipping Ferrara Arc basal thrust, and each one being organized in second-order individual segments. Starting with Late Pliocene times, the Ferrara Arc basal thrust and its splays progressively nucleated and propagated upwards, controlling the development and growth of the foreland-convex Ferrara Arc, and specifically of the MTS first, and of the FTS later on (Figs. 1b and 7b). With the end of the Early Pleistocene, the outer front of the Ferrara Arc reached its present location, and the ongoing NNE-directed compression was mainly accomplished by almost pure shortening along the E-W to WNW-ESE structures of the FTS and by oblique-deformation along the WSW-ENE left-lateral ramp of the MTS.

2 - The internal organization of the FTS is more complex than previously known (Pezzo *et al.*, 2013; Tizzani *et al.*, 2013; Govoni *et al.*, 2014; among many others). In fact, four major individual thrust segments, almost equivalent in size (nearly 25 km long and 15 km wide), can be recognized: Quarantoli, Poggio Rusco, Casaglia, and Sermide (Figs. 7 and 9 and Table 2). Quarantoli and Sermide are nothing else than the Inner and Outer Ferrara thrusts *Auctorum*; Poggio Rusco and Casaglia are up to now undervalued along-strike complexities of the Middle Ferrara Thrust.

3 - The relocated earthquakes, projected at hypocentral depth with standard deviation along

the trace of newly interpreted cross-sections, highlight that the Emilia 2012 sequence mainly activated the FTS and only very subordinately the MTS. On May 20, the Poggio Rusco segment released the strongest event, EQ1, but also the Casaglia segment was activated, producing at least one event with M_W>5.0 (Table 2). From May 20 to 28, the seismic release was mainly concentrated on the Poggio Rusco-Casaglia alignment at depths between 4 and 9 km. From May 29 onwards, it shifted westwards, activating the *en echelon* Quarantoli segment and producing EQ2, at a hypocentral depth of about 9 km. The EQ2 aftershock sequence (May 29 - June 12 in Fig. 7) was mainly concentrated on a low-angle patch of the Quarantoli segment, at depths between 6-7 and 10-11 km. Simultaneously, also a patch of the shallower Mirandola Thrust, underlying the Cavone field and located at depths of 4.5 to 6.0 km, was activated by microseismicity, as well as by a few more energetic compressional events (e.g., EQ#, M_W 4.4). Therefore, four very distinct individual segments, with different roles and degrees of involvement, were activated during the Emilia 2012 sequence.

4 - In the course of three weeks, the Emilia 2012 sequence covered a large epicentral area, extending, on the average, in a N100° direction with a length of about 50 km and a surface width of about 6-7 km. The huge size of the overall aftershock area when compared with the magnitude of the main events (EQ1, M_W 6.1 and EQ2, M_W 5.8) may be better understood when considering the complexity of the segmentation pattern and the activation of the independent Casaglia source, highlighted in this paper. In historical times, this source was possibly more active than the two other ones (Quarantoli and Poggio Rusco), causing several significant historical earthquakes (Table 2).

5 - The Quarantoli and Poggio Rusco seismogenic patches containing the two more energetic earthquakes of the sequence (e.g., EQ1 and EQ2) are both not only far away from the Cavone reservoir (≥5 km and ≥15 km, respectively) and outside of the region of possible stress variations as computed by Astiz *et al*. (2014), but they are also in no physical contact with the Mirandola Thrust underlying the oil field. A hydraulic connection between the reservoir and the faults that slipped during the two main May 20 and 29 events can be therefore excluded. Conversely, we do not discard the possibility that the shallow minor seismic activity within the Cavone field and the underlying Mirandola segment event may effectively represent a triggered, or even an induced, phenomenon due to the C14 injection-related Coulomb stress increase. Therefore, we wonder if, in the future, injection-related net pressure variations in the Cavone oil field might indeed play a role in triggering earthquake activities associated with shearing process along the northern half of the WSW-ENE Mirandola left lateral ramp (e.g., Fabbrico segment), which lies close to the Cavone reservoir and has been aseismic since historical times.

6 - The recognition, in this paper, of a seismogenic pattern involved in the Emilia 2012 sequence more complex than proposed even in the very recent literature (Vannoli *et al*., 2014), together with the parameterization of the identified individual fault segments, brings additional and more detailed information to the characterization of the seismotectonic setting of the Ferrara Arc, as a basic tool for improved seismic hazard evaluations of the Padan region.

Acknowledgments. This work was supported by G. d'Annunzio University funds to G. Lavecchia and by INGV-DPC funds to G. Costa (Convenzione INGV-DPC 2014/2015 Progetti sismologici - Progetto S1: "*Miglioramento delle conoscenze per la definizione del potenziale sismogenico*). Many thanks to G. Milana and M. Menichetti for critically reviewing our paper.

REFERENCES

Anelli L., Mattavelli L. and Pieri M.; 1996: *Structural-stratigraphic evolution of Italy and its petroleum systems*. In: Ziegler P.A. and Horvath F. (eds), Peri-Tethys Memoir 2, Structure and prospects of alpine basins and forelands, Memoires du Museum National d'Histoire Naturelle, **170**, 455-483.

Astiz L., Dieterich J.H., Frohlich C., Hager B.H., Juanes R. and Shaw J.H.; 2014: *On the potential for induced seismicity at the Cavone oilfield: analysis of geological and geophysical data, and geomechanical modeling*. Report for Laboratorio di Monitoraggio Cavone, Italy, 139 pp.

Bertello F., Fantoni R., Franciosi R., Gatti V., Ghielmi M. and Pugliese A.; 2010: *From thrust-and-fold belt to foreland: hydrocarbon occurrences in Italy*. In: Vining B.A. and Pickering S.C. (eds), Proc. 7th Petroleum Geology Conference series, vol. **7**, pp. 113-126.

Bignami C., Burrato P., Cannelli V., Chini M., Falcucci E., Ferretti A., Gori S., Kyriakopoulos C., Melini D., Moro M., Novali F., Saroli M., Stramondo S., Valensise G. and Vannoli P.; 2012: *Coseismic deformation pattern of the Emilia 2012 seismic sequence imaged by Radarsat-1 interferometry*. Ann. Geophys., **55**, 789-795, doi:10.4401/ag-6157.

Boccaletti M., Corti G. and Martelli L.; 2011: *Recent and active tectonics of the external zone of the northern Apennines (Italy)*. Int. J. Earth Sci., **100**, 1331-1348.

Bonini L., Toscani G. and Seno S.; 2014: *Three-dimensional segmentation and different rupture behavior during the 2012 Emilia seismic sequence (northern Italy)*. Tectonophysics, **630**, 33-42.

Bragato P.L., Sugan M., Augliera P., Massa M., Vuan A. and Saraò A.; 2011: *Moho reflection effects in the Po Plain (northern Italy) observed from instrumental and intensity data*. Bull. Seismol. Soc. Am., **101**, 2142-2152.

Burrato P., Vannoli P., Fracassi U., Basili R. and Valensise G.; 2012*: Is blind faulting truly invisible? Tectonic-controlled drainage evolution in the epicentral area of the May 2012, Emilia-Romagna earthquake sequence (northern Italy)*. Ann. Geophys., **55**, 525-531, doi:10.4401/ag-6182.

Carminati E. and Vadacca L.; 2010: *Two- and three-dimensional numerical simulations of the stress field at the thrust front of the northern Apennines, Italy*. J. Geophys. Res., **115**, B12425, doi:10.1029/2010JB007870.

Carminati E., Scrocca D. and Doglioni C.; 2010: *Compaction-induced stress variations with depth in an active anticline: northern Apennines, Italy*. J. Geophys. Res., **115**, 1-17.

Casero P.; 2004: *Structural setting of petroleum exploration plays in Italy*. In: Crescenti V., D'Offizi S., Merlino S. and Sacchi L. (eds), Geology of Italy. Special volume of the Italian Geological Society for the IGC, vol. 32, pp. 189-199.

Castelli V., Bernardini F., Camassi R., Caracciolo C.H., Ercolani E. and Postpischl L.; 2012: *Looking for missing earthquake traces in the Ferrara-Modena plain: an update on historical seismicity.* Ann. Geophys., **55**, 519-524, doi:10.4401/ag-6110.

Cesca S., Braun T., Maccaferri F., Passarelli L., Rivalta E. and Daham T.; 2013a: *Source modelling of the M 5-6 Emilia-Romagna, Italy, earthquakes (2012 May 20-29)*. Geophys. J. Int., **193**, 1658-1672.

Cesca S., Dost B. and Oth A.; 2013b: *Preface to the special issue* "*Triggered and induced seismicity: probabilities and discrimination*". J. Seismol., **17**, 1-4, doi:10.1007/s10950-012-9338-z.

Chatelain J.; 1978: *Étude fine de la sismicité en zone de collision continentale à l'aide d'un réseau de stations portables: la région Hindu-Kush Pamir*. Ph.D. thesis, Université Paul Sabatier, Toulouse, France.

Chiarabba C., De Gori P., Improta L., Lucente F.P., Moretti M., Govoni A., Di Bona M., Margheriti L., Marchetti A. and Nardi A.; 2014: *Frontal compression along the Apennines thrust system: the Emilia 2012 example from seismicity to crustal structure*. J. Geodyn., **82**, 98-109.

Chiarabba C., De Gori P. and Mele F.; 2015: *Recent seismicity of Italy: active tectonics of the central Mediterranean region and seismicity rate changes after the Mw 6.3 L'Aquila earthquake*. Tectonophysics, **638**, 82-93.

CNR - P.F. Geodinamica; 1990: *Structural model of Italy 1:500.000 and gravity map, sheet n. 1-6*. Quad. Ric. Sci., 114, S.EL.CA., Firenze, Italy.

Convertito V., Catalli F. and Emolo A.; 2013: *Combining stress transfer and source directivity: the case of the 2012 Emilia seismic sequence*. Sci. Report-UK, **3**, 3114, doi:10.1038/srep03114.

Costa G., Panza G.F., Suhadolc P. and Vaccari F.; 1992: *Zoning of the Italian region with synthetic seismograms computed with known structural and source information*. In: Proc. 10th World Conf. Earthquake Eng., Madrid, Spain, pp. 435-438.

de Nardis R., Filippi L., Costa G., Suhadolc P. and Lavecchia G.; 2014: *Strong motion recorded during the Emilia 2012 thrust earthquakes (northern Italy): a comprehensive analysis*. Bull. Earthquake Eng., **12**, 2117-2145, doi:10.1007/s10518-014-9614-0.

Devoti R.; 2012: *Combination of coseismic displacement fields: a geodetic perspective*. Ann. Geophys., **55**, 781-787, doi:10.4401/ag-6119.

Devoti R., Esposito A., Pietrantonio G., Pisani A.R. and Riguzzi F.; 2011: *Evidence of large scale deformation patterns from GPS data in the Italian subduction boundary*. Earth Planet. Sci. Lett., **311**, 230-241.

DISS Working Group; 2015: *Database of Individual Seismogenic Sources (DISS). Version 3.2.0: a compilation of potential sources for earthquakes larger than M 5.5 in Italy and surrounding areas*, doi:10.6092/INGV.IT-DISS3.2.0., <diss.rm.ingv.it/diss/>.

Galli P., Castenetto S. and Peronace E.; 2012: *The MCS macroseismic survey of the Emilia 2012 earthquakes*. Ann. Geophys., **55**, 663-672, doi:10.4401/ag-6163.

Gallo A., Costa G. and Suhadolc P.; 2014: *Real-time automatic moment magnitude estimation*. Bull. Earthquake Eng., **12**, 185-202.

Ghielmi, M., Minervini M., Nini C., Rogledi S., Rossi M. and Vignolo A.; 2010: *Sedimentary and tectonic evolution in the eastern Po-Plain and northern Adriatic Sea area from Messinian to Middle Pleistocene (Italy)*. Rendiconti Lincei-Scienze Fisiche e Naturali, **21**, 131-166.

Gorini A., Nicoletti M., Marsan P., Bianconi R., De Nardis R., Filippi L., Marcucci S., Palma F. and Zambonelli E.; 2010: *The Italian strong motion network*. Bull. Earthquake Eng., **8**, 1075-1090.

Govoni A., Marchetti A., De Gori P., Di Bona M., Lucente F.P., Improta L., Chiarabba C., Nardi A., Margheriti L., Agostinetti N.P., Di Giovambattista R., Latorre D., Anselmi M., Ciaccio M.G., Moretti M., Castellano C. and Piccinini D.; 2014: *The 2012 Emilia seismic sequence (northern Italy): imaging the thrust fault system by accurate aftershocks location*. Tectonophys., **622**, 44-55.

Grasso J.R.; 1992: *Mechanism of seismic instability induced by the recovery of hydrocarbons*. Pure Appl. Geophys., **139**, 507-534.

Grasso J.R. and Sornette D.; 1998*: Testing self-organized criticality by induced seismicity*. J. Geophys. Res., **103,** 29965-29987.

International Commission on Hydrocarbon Exploration and Seismicity in the Emilia region (ICHESE); 2014: *Report on the Hydrocarbon Exploration and Seismicity in Emilia Region,* 213 pp., <mappegis.regione.emilia-romagna.it/gstatico/documenti/ICHESE/ICHESE>.

ISIDe Working Group INGV; 2015*: Italian Seismological Instrumental and parametric Database*. INGV, Roma, Italy, <iside.rm.ingv.it/iside>.

Lahr J.C.; 1999: *HYPOELLIPSE Y2K: a computer program for determining local earthquakes hypocentral parameters, magnitude, and first-motion pattern*. U.S. Geological Survey, Open-file Report 99-23, USA, 112 pp., <greenwood.cr.usgs.gov/pub/open-file-reports/ofr-99-0023>.

Lavecchia G., de Nardis R., Cirillo D., Brozzetti F. and Boncio P.; 2012: *The May-June 2012 Ferrara Arc earthquakes (northern Italy): structural control of the spatial evolution of the seismic sequence and of the surface pattern of co-seismic fractures*. Ann. Geophys., **55**, 533-540, doi:10.4401/ag-6173.

Malagnini L., Herrmann R.B., Munafò I., Buttinelli M., Anselmi M., Akinci A. and Boschi E.; 2012: *The 2012 Ferrara seismic sequence: regional crustal structure, earthquake sources, and seismic hazard*. Geophys. Res. Lett., **39**, L19302, doi:10.1029/2012GL053214.

Manighetti I, Caulet C., De Barros L., Perrin C., Cappa F. and Gaudemer Y.; 2015: *Generic along-strike segmentation of Afar normal faults, east Africa: implications on fault growth and stress heterogeneity on seismogenic fault planes*. Geochem. Geophys. Geosyst., **16**, 443-467.

Martelli L. and Molinari F.C.; 2008: *Studio geologico finalizzato alla ricerca di potenziali serbatoi geotermici nel sottosuolo del comune di Mirandola*. Regione Emilia-Romagna, Servizio geologico, sismico e dei suoli, Bologna, Italy, 26 pp.

Marzorati S., Carannante S., Cattaneo M., D'Alema E., Frapiccini M., Ladina C., Monachesi G. and Spallarossa D.; 2012: *Automated control procedures and first results from the temporary seismic monitoring of the 2012 Emilia sequence*. Ann. Geophys., **55**, 575-581, doi:10.4401/ag-6116.

Massa M., Carannante S., Lovati S., D'Alema E., Moretti M., Piccinini D., Monachesi G., Cattaneo M. and Augliera P.; 2013: *Relocated seismicity in the Po Plain, in Project S1: base-knowledge improvement for assessing the seismogenic potential on Italy.* Scientific Report - I Semester. Agreement INGV-DPC 2012-2013, pp. 52-58.

Massoli D., Koyi H.A. and Barchi M.R.; 2006: *Structural evolution of a fold and thrust belt generated by multiple décollements: analogue models and natural examples from northern Apennines (Italy*). J. Struct. Geol., **28**, 185-199.

Milana G., Bordoni P., Cara F., Di Giulio G., Hailemikael S. and Rovelli A.; 2014: *1D velocity structure of the Po River plain (northern Italy) assessed by combining strong motion and ambient noise data*. Bull. Earthquake Eng., **12,** 2195-2209.

Montone P., Mariucci M.T. and Pierdominici S.; 2012: *The Italian present-day stress map*. Geophys. J. Int., **189**, 705-716.

Mulargia F. and Bizzarri A.; 2014: *Anthropogenic triggering of large earthquakes*. Nature.com webcasts, Scientific Report, **4**, 6100, doi:10.1038/srep06100.

Nardon S., Marzorati D., Bernasconi A., Cornini S., Gonfalini M., Mosconi S., Romano A. and Terdich P.; 1990: *Cavone oil field (Italy): an example of the application of integrated methodologies to reservoir characterization.* Mem. Soc. Geol. It., **45**, 791-805.

Pettenati F., Sirovich L. and Cavallini F.; 2013: *Contributo per la sismotettonica della Pianura Padana, dai terremoti del 1570 e del 2012*. In: Abstract 32nd Convegno Nazionale Gruppo Nazionale Geofisica Terra Solida, Trieste, Italy, Vol. 3, pp. 182-186.

Pezzo G., Merryman J.P., Boncori C., Tolomei S., Salvi S., Atzori A., Antonioli E., Trasatti F., Novali E., Serpelloni L., Candela L. and Giuliani R.; 2013: *Coseismic deformation and source modelling of the May 2012 Emilia (northern Italy) earthquakes*. Seismol. Res. Lett., **84**, 645-655.

Picotti V. and Pazzaglia F.J.; 2008: *A new active tectonic model for the construction of the northern Apennines mountain front near Bologna (Italy)*. J. Geophys. Res., **113**, B08412, doi:10.1029/2007JB005307.

Pondrelli S., Salimbeni S., Perfetti P. and Danecek P.; 2012: *Quick regional centroid moment tensor solutions for the Emilia 2012 (northern Italy) seismic sequence*. Ann. Geophys., **55**, 615-621, doi:10.4401/ag-6146.

Rovida A., Camassi R., Gasperini and Stucchi M.; 2011: *CPTI11, the 2011 version of the Parametric Catalogue of Italian Earthquakes*. Milano, Bologna, Italy, doi:10.6092/INGV.IT-CPTI11, <emidius.mi.ingv.it/CPTI>.

Saraò A. and Peruzza L.; 2012: *Fault-plane solutions from moment-tensor inversion and preliminary Coulomb stress analysis for the Emilia Plain*. Ann. Geophys., **55,** 647-654, doi:10.4401/ag-6134.

Scognamiglio L., Margheriti L., Mele F.M., Tinti E., Bono A., De Gori P., Lauciani V., Lucente F.P., Mandiello A.G., Marcocci C., Mazza S., Pintore S. and Quintiliani M.; 2012: *The 2012 Pianura Padana Emiliana seimic sequence: locations, moment tensors and magnitudes*. Ann. Geophys., **55**, 549-559, doi:10.4401/ag-6159.

Scrocca D., Carminati E., Doglioni C. and Marcantoni D.; 2007: *Slab retreat and active shortening along the central-northern Apennines*. In: Lacombe O., Lave J., Roure F. and Verges J. (eds), Thrust belts and foreland basins: from fold kinematics to hydrocarbon systems. Frontiers in Earth Sciences, pp. 471-487.

Selvaggi G., Ferulano F., Di Bona M., Frepoli A., Azzara R., Basili A., Chiarabba C., Ciaccio M.G., Di Luccio F., Lucente F.P., Margheriti L. and Nostro C.; 2001: *The M_W 5.4 Reggio Emilia 1996 earthquake: active compressional tectonics in the Po Plain, Italy*. Geophys. J. Int., **144**, 1-13.

Tertulliani A., Arcoraci L., Berardi M., Bernardini F., Brizuela B., Castellano C., Del Mese S., Ercolani E., Graziani L., Maramai A., Rossi A., Sbarra M. and Vecchi M.; 2012: *The Emilia 2012 sequence: a macroseismic survey*. Ann. Geophys., **55**, 679-687, doi:10.4401/ag-6140.

Tizzani P., Castaldo R., Solaro G., Pepe S., Bonano M., Casu F., Manunta M., Manzo M., Pepe A., Samsonov S., Lanari R. and Sansosti E.; 2013*: New insights into the 2012 Emilia (Italy) seismic sequence through advanced numerical modeling of ground deformation InSAR measurements*. Geophys. Res. Lett., **40**, 1971-1977, doi:10.1002/grl.50290, 2013.

Toscani G., Burrato P., Di Bucci D., Seno S. and Valensise G.; 2009: *Plio-Quaternary tectonic evolution of the northern Apennines thrust fronts (Bologna-Ferrara section, Italy): seismotectonic implications*. Ital. J. Geosci., **128**, 605-613.

Vannoli P., Burrato F. and Valensise L.; 2014: *The seismotectonics of the Po Plain (northern Italy): tectonic diversity in a blind faulting domain*. Pure Appl. Geophys., **172,** 1105-1142, doi:10.1007/s00024-014-0873-0.

Ventura G. and Di Giovambattista R.; 2013: *Fluid pressure, stress field, and propagation style of coalescing thrusts from the analysis of the 20 May 2012 Ml 5.9 Emilia earthquake (northern Apennines, Italy)*. Terra Nova, **25**, 72-78.

ViDEPI Project, 2014: *Visibility of Petroleum Exploration Data in Italy*. Ministero Sviluppo Economico, Assomineraria, Societa' Geologica Italiana, Roma, Italy, <unmig.sviluppoeconomico.gov.it/videpi/en/pozzi/pozzi.asp>.

Wells D.L. and Coppersmith K.J.; 1994: *New empirical relationships among magnitude, rupture length, rupture width, rupture area, and surface displacement*. Bull. Seismol. Soc. Am., **84**, 974-1002.

Zambonelli E., de Nardis R., Filippi L., Nicoletti M. and Dolce M.; 2011: *Performance of the Italian strong motion network during the 2009, L'Aquila seismic sequence (central Italy)*. Bull. Earthquake Eng., **9**, 39-65.

Zollo A., De Matteis R., Capuano P., Ferulano F. and Iannaccone G.; 1995: *Constraints on the shallow crustal model of the northern Apennines (Italy) from the analysis of micro-earthquake seismic records*. Geophys. J. Int., **120**, 646-662.

Corresponding author: Giusy Lavecchia
Università degli Studi "G. d'Annunzio"
Via dei Vestini 30, 66100 Chieti Scalo (CH) Italy
Phone: +39 0871 3556414; fax: +39 0871 3556454; e-mail: glavecchia@unich.it